Hochschule für Angewandte Wissenschaften Hamburg

Hamburg University of Applied Sciences

Projekt

Department Fahrzeugtechnik und Flugzeugbau

A handbook method for the estimation of power requirements for electrical de-icing systems

Verfasser: Oliver Meier

Prüfer: Prof. Dr.-Ing. Dieter Scholz, MSME

DEPARTMENT OF AUTOMOTIVE AND AERONAUTICAL ENGINEERING

Berechnung und Abschätzung der Leistungsanforderungen von De-Icing Systemen im Flugzeugentwurf

Aufgabenstellung zum *Projekt 2* gemäß Prüfungsordnung

Hintergrund

Bei der Berechnung des Leistungsbedarfs zur Enteisung von Flugzeugen werden im kommerziellen Bereich Softwaretools eingesetzt, welche auf der Methode der numerischen Strömungsmechanik (CFD –Verfahren) beruhen. Da der Flugzeugentwurf auf der Vereinfachung komplexer Berechnungsverfahren beruht, ist es erforderlich derartige Berechnungsverfahren durch einen empirischen Ansatz zu vereinfachen. Innerhalb dieser Projektarbeit soll eine Methode erarbeitet werden, welche die Berechnung des Leistungsbedarfs zur Enteisung von Flugzeugen durch eine einfache Handrechenmethode wiedergibt. Ferner sollen Untersuchen durchgeführt werden, welche durch Variation bestehender De-Icing Systeme eine Betrachtung des Leistungsbedarfs für die Enteisung aufweisen.

Aufgabe

- Literaturrecherche bezüglich kommerziell verwendeter Softwaretools zur Bestimmung des Leistungsbedarfs von Enteisungssystemen in Flugzeugen.
- Entwicklung eines Berechnungsschemas zur Leistungsbestimmung von Enteisungssystemen in Flugzeugen.
- Bestimmung des Auslegungspunkts von De-Icing Systemen unter Berücksichtigung der Flugmission und den damit verbundenen äußeren Einflüssen.
- Durchführung einer Fallstudie an Hand von bestehenden Flugzeugmustern mit dem Ziel der Verifikation des Berechnungsschemas und dem Entwurf einer vereinfachten Handrechenmethode für den Flugzeugentwurf.
- Entwicklung eines Konzeptvorschlags für ein De-Icing System durch Variation bestehender De-Icing Methoden.

Die Ergebnisse sollen in einem Bericht dokumentiert werden. Bei der Erstellung des Berichtes sind die entsprechenden DIN-Normen zu beachten.

Abstract

This project shows a handbook method to calculate the energy need for electrical de-icing systems for a first approximation in sizing of aircraft systems. The task of de-icing systems is to avoid hazardous ice accretions which could cause great problems especially during take-off and climb. Those accretions influence the flight physics negatively by reducing the lift and altering the flight characteristics. This work gives an overall view about the icing physics and weather conditions where icing occurs with an eye on the EASA CS 25 certification specification for icing conditions. Furthermore the problem to predict such accretions and deduce the needed power for de-icing systems is reviewed by showing the computer codes and programs based on CFD which are mainly used today. The quality and problems of the computed results are also shown in the summary.

The paper for the DLRK 2010 (**Appendix A and B** part of this project) shows a simplified method to determine the energy need for an electrical de-icing system by establishing the mass and heat balance at on design point on the airfoil (2-D effects only). The results are compared with a state-of-the-art handbook method published by the SAE to validate the results. The calculated example is based on the parameters of a Boeing B787 (**Appendix D**). The results show that the simplified method produces quick and quite good results.

7 ca a YfWJU¨i gY¨glf]Wñmidfc\ ]V]hYX"

Mci f¨fYei Ygh'a UmiVY¨X]fYWñYX¨hc.

DfcZ¨8 f"!=b["8]YhYf¨GW\ c`n¨AGA9
9 !A U]`gYY.\ Hd.#k k k 'DfcZGW\ c`n"XY

8 ck b`cUX¨h\ ]g¨Z]¨Y¨Z]ca .\ Hd.#6 ]V¨]c]\ Y_"DfcZGW\ c`n"XY

Contents

List of Figures

List of Tables

Nomenclature

See the introduction of the paper in Appendix A

List of Abbreviations

AIR   Aerospace Information Report
CFD   Computer fluid dynamics
CS   Certification Specification
EASA   European Aviation Safety Agency
FAR   Federal Aviation Regulations
NASA   Aeronautics and Space Administration
ONERA   Office National d'Etudes et Recherches Aérospatiales
RAE   Royal Aircraft Establishment
URL   Universal Resource Locator
WWW   World Wide Web

1 Introduction

Clouds contain supercooled water under meteorological icing conditions. With the aircraft flying trough, supercooled water droplets impinge on aircraft leading edges. The impinging water droplets freeze because they receive the necessary energy input to overcome the latent heat for the phase change. A layer of ice is forming on leading edges and continuing to grow if the respective surface remains unprotected. Ice accumulations on an aircraft are extremely hazardous dependent on the degree of coverage, the shape, size and texture of the ice growth, and the specific location on the surface of the airfoil (**Al-Khalil 2007**). Flow distribution around the airfoil changes. Those effects will result in a decrease of lift and angle of attack margin to stall while aerodynamic drag increases. Ice protection principals can be generally classified into anti-icing or deicing. Where antiicing systems keep the surface to be protected completely ice free, ice build-ups are allowed to form to get periodical shed with the application of a deicing system. Anti-icing can be achieved by evaporating all of the impinging water (evaporative anti-icing) or by allowing to run back and freeze on no critical areas (running-wet anti-icing). Deicing requires less power than anti-icing because of a short but periodic energy input in contrast to a continuous one. For jet aircraft, de-icing or anti-icing is classically done with pneumatic power. Pneumatic power is taken as bleed air from the aircraft engines and holds sufficient power. So called boots (boot surfaces) remove ice accumulations mechanically by alternately inflating and deflating tubes. Thus, during the off-time of the system, ice is forming, which is then shed periodically by destroying the bond between the ice and the protected surface either through mechanical or thermal energy inputs. Therefore computer based tools are introduced which helps to verify aircraft icing process and a closer look to the overall icing process is given.

1.1 Motivation

De-icing or anti-icing is classically done with pneumatic power. Pneumatic power is taken as bleed air from the aircraft engines and holds sufficient power. Electrical power in contrast is taken from generators on board the aircraft. Generators can provide considerably less power than a pneumatic system. Electrical de-icing of larger components or surfaces causes hence a problem due to high power demands.

Boeing predicts (**Sinnett 2010**) that no-bleed systems are able to save fuel and enhance the operational efficiency of commercial aircrafts especially of the new Boeing 787. So handbook methods should prove their benefits in early phases of a project during trade off studies where fist decisive decisions are taken. Those first steps are vital and rule the whole design process where later changes and mismatches cost plenty of money. Hence a quick and easy to use

handbook method is required. Yields that equations from the thermodynamic first principals combined with SI units are chosen to ensure an international and clear approach.

1.2　Definitions

ANTI-ICING
is the prevention of ice build-up on the protected surface, either by evaporating the impinging water or by allowing it to run back and freeze on noncritical areas
(**AIR 1168/4,** p. 6).

CFD – Computer fluid dynamics

CONTINUOUS MAXIMUM ICING
The continuous maximum icing condition is characterized by exposure to moderate-to-low liquid water content for an extended period of time. It is applicable to those components such as wing ant tail surfaces that are affected by continuous flight in icing conditions but which can tolerate brief and intermittent encounters with conditions of greater severity
(**AIR 1168/4**, p. 29).

CLEAR ICE
A glossy, clear, or translucent ice formed by relatively slow freezing of large supercooled droplets. The large droplets spread out over the airfoil prior to complete freezing, forming a sheet of clear ice. Although clear ice is expected mostly with temperatures between 32 and 14 degrees Fahrenheit, it does occur at temperatures as cold as -13 degrees Fahrenheit.
(**Bragg 2002**)

DEICING
 is the periodic shedding, either by mechanical or thermal means, of small ice build-ups by destroying the bond between the ice and protected surface (**AIR 1168/4**, p. 6).

ICING
Any deposit or coating of ice on an object that is caused by impingement and freezing of liquid hydrometeors (also called riming). (**Bragg 2002)**

ICING CLOUD
Icing clouds are those containing supercooled water droplets in sufficient concentration to produce ice on an aircraft surface (**AIR 1168/4**, p. 5).

INTERMITTENT MAXIMUM ICING

The intermittent maximum icing condition is characterized by exposure to high liquid water contents for a short period, usually superimposed upon the continuous maximum. It is applicable to those components such as engine inlets and guide vanes where ice accretions, even though slight and of short duration, cannot be tolerated
(**AIR 1168/4**, p. 29).

LATENT HEAT

The heat released or absorbed per unit mass by a system in a change of phase.
(Bragg 2002)

LIQUID WATER CONTENT

The total mass of water contained in all the liquid cloud droplets within a unit volume of cloud. Units of LWC are usually grams of water per cubic meter of air (g/m3).
(Bragg 2002)

LIQUID WATER CONTENT (LWC)

The LWC is the mass of supercooled water per volume (**Scholz 2007**, p. 9-3).

LOCAL WATER CATCH

is the point-by-point distribution of water (or ice), in kg/s/m² surface area, over the impingement area (**AIR 1168/4**, p. 6).

MEAN EFFECTIVE DIAMETER (MED)

The droplet diameter which divided the total water volume present in the droplet distribution in half, i.e., half the water volume will be in larger drops and half the volume in smaller drops. The value is calculated based on an assumed droplet distribution. **(Bragg 2002)**

MEAN VOLUMETRIC DIAMETER (MVD)

The droplet diameter which divided the total water volume present in the droplet distribution in half, i.e., half the water volume will be in larger drops and half the volume in smaller drops. The value is calculated based on an assumed droplet distribution. **(Bragg 2002)**

NASA

The National Aeronautics and Space Administration is an Executive Branch agency of the United States government, responsible for the nation's civilian space program and aeronautics and aerospace research.

ONERA

Onera (Office National d'Etudes et Recherches Aérospatiales) is the French national aerospace research center. It is a public research establishment, with eight major facilities in France

RAE

The Royal Aircraft Establishment RAE, was a British research establishment, known by several different names during its history.

RIME

A white or milky granular deposit of ice formed by the rapid freezing of supercooled water drops as they impinge on an exposed object. **(Bragg 2002)**

SUPERCOOLED WATER

Liquid water below 0 °C that turns instantly into ice due to any small disturbance encountered (such as the interaction with the aircraft). Below -40 °C all supercooled water will be frozen (**Scholz 2007**, p. 9-2).

SUPERCOOLING

The reduction in the temperature of any liquid below its melting point without freezing. **(Bragg 2002)**

WET RUNWAY

A runway is considered wet when the runway surface is covered with water, or equivalent, less than or equal to 3 mm or when there is sufficient moisture on the runway surface to cause it to appear reflective, but without significant areas of standing water. **(Bragg 2002)**

1.3   Aim of the study

This project tries to show up icing process, -condition, design point and the estimation of power requirements for electrical de-icing systems. Furthermore this project should improve handbook methods, to show program codes, used industrial tools for ice accretion / energy prediction and to give a overall understanding of the icing process. The handbook method from this project contributes to the preliminary sizing of electrical de-icing systems. It hence simplifies the preparation of trade-off studies.

1.4   Structure of the project

The project is structured into 7 chapters and 3 Appendix as follows:

Chapter 2   Summary report of the handbook method which can be seen in detail in Appendix A.

Chapter 3   This chapter gives a short overview about the structure of the paper.

Chapter 4   This chapter shows up general mathematical models.

Chapter 5   In this chapter a short overview of common used computer codes to predication icing conditions is given.

Chapter 6   Here the most common basic icing conditions and icing principals are explained.

Chapter 7   This chapter explains shortly an alternative Low Power Ice Protection Systems for future aircraft designs.

Appendix A   DLRK 2010 paper: A HANDBOOK METHOD FOR THE ESTIMATION OF POWER REQUIREMENTS FOR ELECTRICAL DE-ICING SYSTEMS

Appendix B   DLRK 2010 power point presentation

Appendix C   CANISE code improvement

Appendix D   Geometry Report B787

Appendix E   Excelsheet: Calculation of De-Icing Power

1.5   Overview of the literature

For the very special topic de-icing calculation most of the literature or papers are found by using the search engine www.google.de. The used papers are free available and can be downloaded from the URL listed in the references.

Some books like **Incropera 2007** or the lector note from **Scholz 1997** could be found in the library of the HAW Hamburg and the personal homepage "www.profscholz.de" (students only).

Literature contains equations dealing with energy mass balance and models to describe the ice accretions on airfoils:
- **Bragg 2002**
- **Incropera 2007**
- **La Burthe 2010**
- **SAE 1990**
- **Sherif 1997**

This references deals with CFD icing codes and their mathematical models:
- **Al-Khalil 1997**
- **Gehrer 1999**
- **Habashi 2002**
- **Habashi 2004**
- **LTH 2008**
- **Paraschivoiu 2001**
- **Wright 1997**

This references shows up general icing conditions, parameters and de-icing systems:
- **Al-Khalil 2007**
- **Bigarré 2003**
- **Klimedia 2010**
- **Scholz 2007**
- **Sinnett 2010**
- **Majed 2006**

This article points out the special electrical design of the Boeing 787:
- **CW 2008**

Finally the Certification specifications which defines the essential legal provisions for aircraft construction:
- **EASA 2008**

2   Summary of the report

"Power by Wire", the "All Electric Aircraft" or the "More Electric Aircraft" – topics that have been discussed for years. However the application of these concepts in civil aviation was decelerated by the fact that in an "All Electric Aircraft" not only the power generation but also all the consumers have to be electrical. For example the introduction of electrical primary flight controls, braking systems or de-icing systems has seen many challenges and their overall economical benefits were often unclear. In order to prove the benefits of electrical systems, trade-off studies build a solid and inevitable foundation. These trade-off studies are required in the very early phases of an aircraft project. The early phase of a project is characterized by a lack of data and very limited Investigation. Often many system variants have to be checked with a limited amount of engineering man power. Handbook methods, which are usually quick and easy to use are generally a good solution to work with in such a situation. The aim of this paper is for the estimation of power requirements for electrical de-icing systems to

- review and comment on state-of-the-art approaches
- review and improve handbook methods

as a contribution to support the preliminary sizing of these systems and hence to simplify the preparation of trade-off studies. De-icing or anti-icing is classically done with pneumatic power. Pneumatic power is taken as bleed air from the aircraft engines and holds sufficient power. Electrical power in contrast is taken from generators on board the aircraft. Generators can provide considerably less power than a pneumatic system. Electrical de-icing of larger components or surfaces hence causes a problem due to high power demands. Electrical de-icing is only possible with surfaces that are just heated during some time intervals (cycling heating) just melt the bonding contact area of the ice and with permanently heated parting strips ensuring separation of the ice layers, which are finally carried away by the air stream.

In **appendix A** this paper, presented on the DLRK 2010 (presentation in **appendix B**) summarize a short heater overview and a capable method for the power estimation of electrical powered icing systems. This study should point out that electrical deicing handbook methods are able to estimate energy requirements during trade-off studies. The icing process of airfoils depends on many physical fundamentals. To gain exact results for final deicing layouts many complex equations have to be considered and of course empirical experiences and data have to determine. Ice protection can either be accomplished by anti-icing, deicing or by a combination of both (referred to as hybrid). Where anti-icing systems keep the surface completely ice free, ice build-ups are allowed to form and to get periodical shed with the application of a deicing system. Deicing requires less power than anti-icing because of a short but periodic energy input that is used to melt the ice-airfoil interface. That way the adhesion of ice build-ups becomes zero and the aerodynamic forces then remove the ice. However,

during the heat-off period the aircraft must be capable of receiving ice accumulations on its wings, engine nacelles etc. The heat off time is tailored to the maximum allowable ice thickness that is lower in the case of high performance aircraft wings.

In order to prevent ice bridging, the stagnation line has to be heated continuously through parting strips. Additionally, chordwise parting strips are necessary to split the surface to be protected into smaller areas. Parting strip power requirements are calculated by means of running-wet antiicing calculation principles because of the continuous heating of the parting strip. Calculation principles are demonstrated according to the method suggested in (**SAE 1990**) as well as through general accepted formula to be found in any common thermodynamic book. The design point for calculations has been set to -18 °C at MSL in continuous maximum icing conditions. In every low power deicing system, either one or both of the following principals are to be found:

- decrease of the continuous heated area (parting strips) and/or
- decrease of the heat-on time (cyclic deicing).

In this report, this methodology has been demonstrated on an electro thermal cyclic deicing system, which provides a very effective and quick method to estimate total power loads (**appendix E**). All stated calculations and formulas provide a generic understanding of the effects that determine electro-thermal cyclic power requirements. The simplest form to calculate the required heat flux is an energy-and-mass-balance for each surface element along an airfoil. It must be kept in mind that the chosen design point is one point on the airfoil dependents on many variables.

So melting 0.05mm ice could not be enough to destroy the bond between ice and airfoil. Furthermore the effect of running back ice especially from the cyclic heated areas is not considered. Ice accretions behind the heated elements cannot be removed and are able to negatively affect the aerodynamic. The achieved results form a first good approximation. It must be kept in mind that if necessary more computing (different design points) has to be performed as shown in this paper. One argument against electric thermal deicing is the high energy consumption per square meter. To maintain a lower energy input the layout mentioned above with parting strips (less zones of running wet anticing) and cyclic deicing (only few zones are heated simultaneously) represent possible solutions. The layout reduces the needed energy from $27.25 \frac{kW}{m^2}$ to $3.61 \frac{kW}{m^2}$. The results was calculated in an excel sheet to gain information about correlations and parameters who alter the results greatly (**appendix E**). The geometry data of the B787 are taken from **appendix D** for first computing.

Rumors about the bleedless engine RR Trent 1000 with 0.5 MW electrical energy output and the amount of 75 kW for the electrical deicing systems leads to the fact that a Boeing 787 requires needs 7.5% of the possible available energy. A reduction in electrical energy results in less generator load and more reserve for other systems. In additions this work gives a short

overview about the icing process and the commercial icing tools and what their performance. The calculation schemes are more complex and use mathematical models to describe the heat and mass flux. A few effects which are not included may be implemented in the future. The CFD technology is seen as a simulation tool. Hand in hand with icing tunnel test and flight test, it has a crucial part to improve safety, reduce the certification time and cut costs. Someday it has the potential to fully replace the other certification tests. Finally there are examples for hazardous weather conditions, icing mechanism/-forms and design points from the EASA to have a better understanding of the icing basics.

3 Handbook method for the estimation of power requirements for electrical de-icing systems

Clouds or visible moisture contain supercooled water under meteorological icing conditions. With the aircraft flying trough, supercooled water droplets impinge on aircraft leading edges. The impinging water droplets freeze because they receive the necessary energy input to overcome the latent heat for the phase change. A layer of ice is forming on leading edges and continues to grow if the respective surface remains unprotected. Ice accumulations on an aircraft are extremely hazardous dependent on the degree of coverage, the shape, size and texture of the ice growth, and the specific location on the surface of the airfoil (**Al-Khalil 1997).** Flow distribution around the airfoil changes. Those effects will result in a decrease of lift and angle of attack margin to stall while aerodynamic drag increases. Additionally the operation of control surfaces might be influenced negatively.

Ice protection principals can be generally classified into anti-icing or deicing. Where anti-icing systems keep the surface to be protected completely ice free, ice build-ups are allowed to form to get periodical shed with the application of a deicing system. Anti-icing can be achieved by evaporating all of the impinging water (evaporative anti-icing) or by allowing to run back and freeze on no critical areas (running-wet anti-icing). Deicing requires less power than anti-icing because of a short but periodic energy input in contrast to a continuous one. Thus, during the off-time of the system, ice is forming, which is then shed periodically by destroying the bond between the ice and the protected surface either through mechanical or thermal energy inputs. For future projects low power requirements are stipulated, as a result deicing would be the preferred method. Combined with cyclic energy input deicing systems have a remarkable low power input. As mentioned in the summary the full method is explained in **Appendix A.** The following content is considered more precisely:

- **INTRODUCTION**
- **AIM, APPROACH AND APPLICATION**
- **CLASSIFICATION OF THERMAL ICE PROTECTION SYSTEMS**
- **CONVENTIONAL THERMAL ICE PROTECTION OF TODAY'S JET AIRCRAFT**
- **PRESENT AND FUTURE CYCLIC ELECTRICAL WING DE-ICING SYSTEMS**
- **ICING FUNDAMENTALS**
- **STATE-OF-THE-ART IN HANDBOOK METHODS**
- **ASSUMPTIONS FOR A HANDBOOK METHOD**
- **SIMPLIFIED WATER CATCH CALCULATION**

- **CALCULATION OF POWER REQUIREMENTS**
  - **Calculation of Power Requirements for Continuously Heated Surfaces**
  - **Calculation of power requirements for cyclic heated surfaces.**
  - **Calculation of Power Requirements for a Generic Heater Layout**
- **ABSOLUTE POWER REQUIREMENTS FOR DE-ICING**
- **SUMMARY AND RECOMMENDATIONS**

4 Used mathematical models

The icing code is used to predict the surface temperature and the amount of runbackwater for given atmospheric conditions. Furthermore the heat flux distribution from an anti-icing device should be determined. The external boundary layer is modeled with an integral method. Velocity and temperature distribution in the water film are estimated using a polynomial approximation. Conduction in the airfoil skin is taken into account with a one-dimensional model. Finally the numerical results are compared with experiment. For first power performance some elementary considerations has to be expressed by mathematical models:

1. External flow region
2. Runback water region
3. Solid region
4. Anti-icing region

4.1 External flow region

The external flow expressed by the streamlines and the droplet trajectories are determined among other thinks by a potential flow field. Each individual droplet trajectory is calculated by integrating the droplet equation of motion with e.g. Runge-Kutta method. The impinging water rate expressed by the water catch efficiency. By using an integral method more vital variables are calculated like: friction coefficient, heat transfer coefficient and the evaporation rate above runback. The flow field is separated into laminar and turbulent boundary layers which are represented by different velocities, friction coefficient and momentum thickness.

4.2 Runback water region

The heat flux coming from the wall and the heat flux lost to the external airflow describes the temperature gradient. The heat flux lost to the airflow includes convection, evaporation and the energy losses to the impinging droplets. The evaporation rate is calculated by using the convection coefficient and the temperature at the surface. The surface of the airfoil is divided into control volume of the length of the panel. Using the mass and energy balance on each control volume the airfoil surface temperature is received. To solve the equation the airfoil wall is divided into control volumes of panel length and of thickness of the airfoil wall. Finally with an iterative procedure the surface temperature and the amount of water that

evaporates are found to give the internal heat transfer coefficient. First an initial surface temperature distribution is used to gain the heat flux from the icing system.

4.3   Solid region

For a thin plate made of material with uniform conductivity k and surface area the temperature across the thickness can be neglected. Only the conduction in direction of the length is considered for the airfoil wall. The airfoil wall spreads the heat coming from the anti-icing system.

4.4   Anti-icing hot air region

The anti-icing hot air region is modeled with a local internal convection coefficient and is considered to be known from calculations or experiments. When the heat transfer coefficient is specified, heat flux coming from the anti-icing system is evaluated with the help of the internal airflow temperature and the local wall temperature. The heat flux from the anti-icing system matching this surface temperature is then assessed again and used to calculate a new surface temperature. The iterative process stops when energy entering the airfoil wall is equal to the energy flux leaving the airfoil wall. Surface temperature depends also highly on the local heat transfer coefficient used. **(Bragg 2002)**

5 Thermal ice protection computer codes

Simulation tools can be graded in 2-D and 3-D software. The 2-D tools like LEWICE (NASA), CANICE-BA (Montreal, Bombardier Aerospace) and methods from Office National d'Études et de Recherches Aérospatiales (ONERA) and Royal Aircraft Establishment (RAE). They focused on ice accretion anticipation. 3-D tools based upon computer fluid dynamics simulations (CFD) used to solve more complex mathematic problems like the ice accretion and airflow for an entire aircraft, swept wings and radomes with e.g. turbulent airflow. Here tools like FENSAP-ICE and 3-D modified derivatives from LEWICE and CANICE-BA exists. It is obvious that different mathematical models have to be used. All solvers perform more or less the same calculation scheme (**Figure 5.1**):

- Describe the flow field
- Analyses the trajectory and water catch
- Calculate the heat transfer
- Measure the ice accretion
- De-Icing power prediction
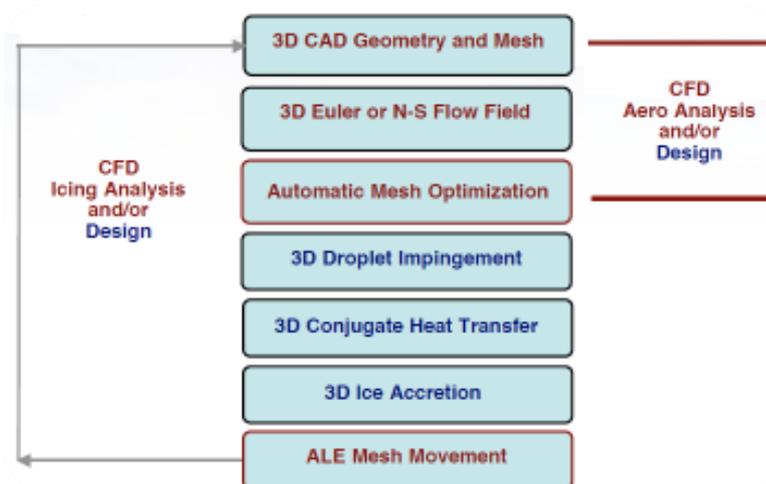
Figure 5.1   Icing scheme as an extension of CFD
(Habashi 2004)

Table 5.1   Used mathematic model

package	2-D solver	3-D solver
flow field	Panel Procedere, Field Method	Reynolds Averaged Navier-Stokes (RANS)
trajectory	Lagrangian particle trajectory analysis	Eulerian particle-tracking

Table 5.1 provides a short overview to separate the solvers. The 2-D solvers use field method or panel procedure to gain information about the adjacent flow field. The trajectories are computed by integration of the equation of motion. Followed by the drag and distribution calculation of water droplets with the law of Stoke and Langmuir D distribution. Finally the heat flux is achieved for every element with the energy mass balance. All these programs are validated by a test in icing tunnels or existing data with very good results. **(Habashi 2002), (LTH 2008)**. They are used to reduce work, cost, support certification and helps in early design stages. So these products can be used to find critical configurations in order to reduce the amount of icing tunnels and natural icing tests.

5.1   FENSAP-ICE CODE PACKAGE

The system intends to combine the design and certification process and furthermore limit the expenses. Critical conditions can be detected more easily which can reducess the span of test size. "Concurrent engineering" combined with information exchange between the aerodynamic and the icing group ensure safe high performance designs and fulfill the step from 3-D CAD based design to start early with icing investigations. To achieve higher performance FENSAP-ICE can be set to a 2-D mode in early design stages. FENSAP-ICE includes different modules to determine the simulation data among the others it uses **RANS** equation to solve the flow field. It has a very modular structure, so every package could be replaced by codes with equivalent functions **(Habashi 2002).** So FENSAP-ICE is separated into packages with different functions (**Figure 5.2**):
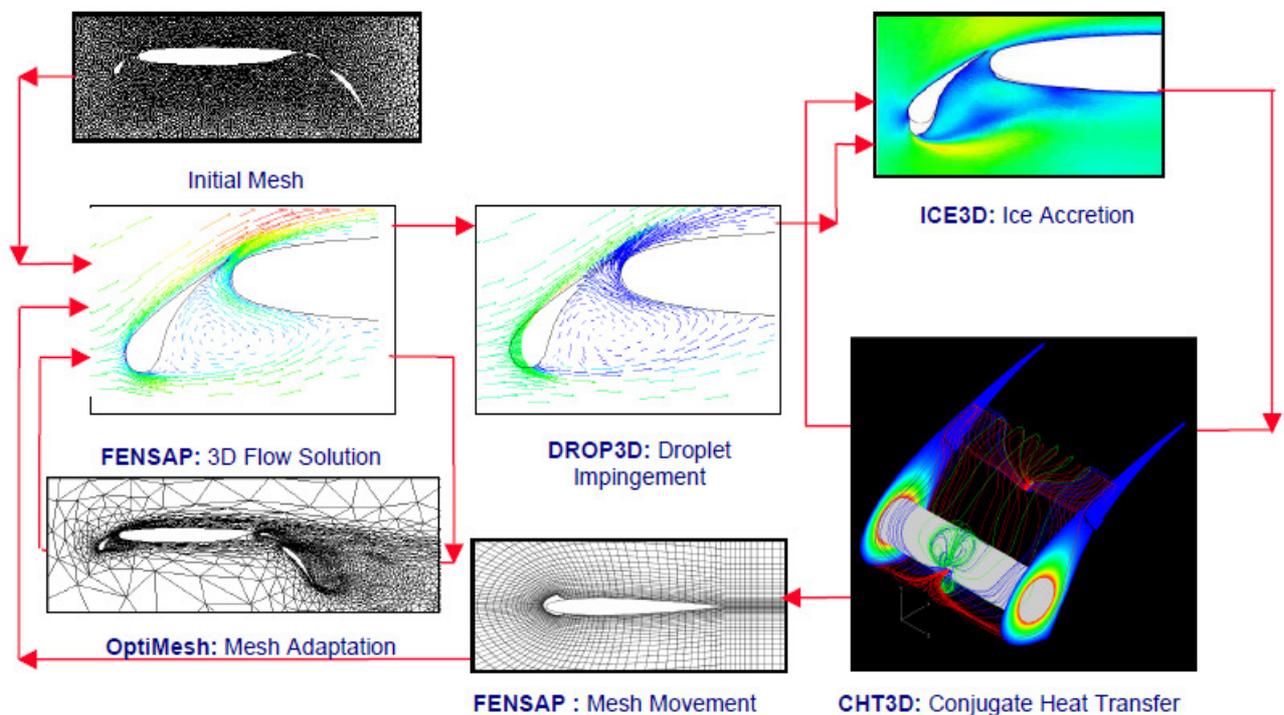
Figure 5.2   Icing accretion flow chart
(Habashi 2002)

5.1.1 FENSAP for the aerodynamic calculation (EULER/Navier-Stokes)

The FENSAP-ICE system has a flow solver and based on FEM which includes low-Re and high-Re turbulence 2-equation models with fixed transition and surface roughness. The code supports mesh movement to minimize remeshing over iced bodies and could also be interfaced to other CFD structured/unstructured flow solvers. (**Figure 5.3**)
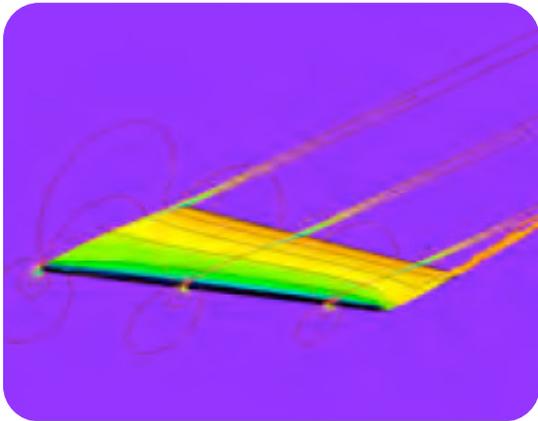
Figure 5.3   Shows the airflow around an wing
(Habashi 2004)

5.1.2 DRPO3D (Eulerian particle tracking)

DROP3D determines the catch efficiency off complex bodies whereby it takes drag, buoyancy and gravitational forces into account. It is possible to simulate supercooled droplets or snow particles (e.g. taxiing aircraft). During computing a field is produced which collect values of LWC, β and droplet velocity everywhere on all walls. The module delimits impingement and shadow zones at the same time and uses the same grid as the flow solver.

5.1.3 ICE3D (finite volume method)

Ice accretion determined an displayed as a 3-D layer on the wing which altered the shape of the wing. The growth module automatically alters the airfoil by using the same grid and droplet solvers. (**Figure 5.4**, **Figure 5.4**)
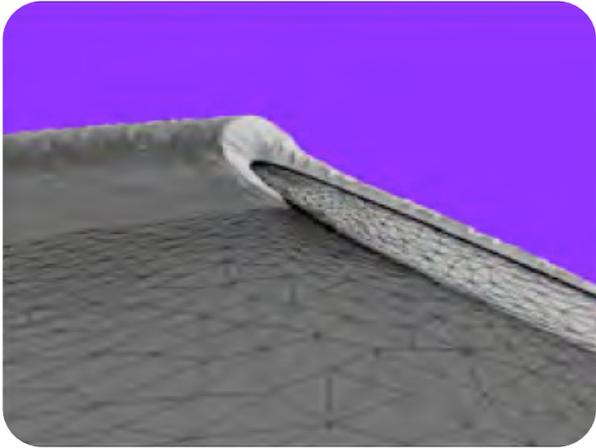
Figure 5.4 Ice accretion at the leading edge
      (Habashi 2004)

5.1.4 CH3D heat transfer interface

With Navier-Stokes solution inside and outside the convection heat transfer is described combined with conduction through the solid medium. (**Figure 5.5**)
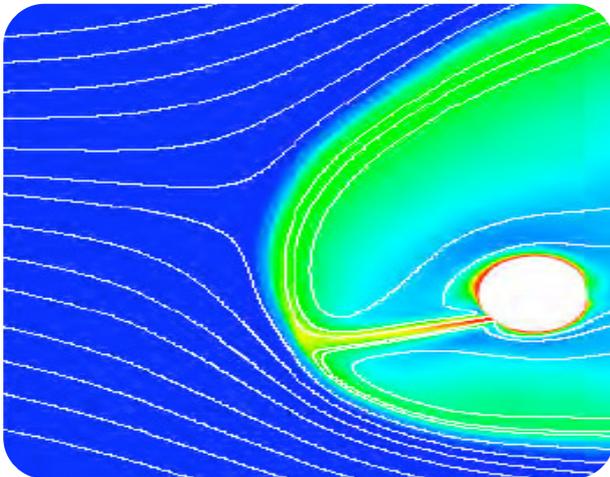
Figure 5.5 Heat distribution inside the leading edge
      (Habashi 2004)

5.1.5 Mesh adaption

Adaption of the mesh increases the CFD fidelity and reduces mesh generation efforts. If any solution error accurse mesh points are adapt, refines, coarsens and swaps edges. Yields highly stretched grids, allowing solution with a reduced number of points. (**Figure 5.6**)
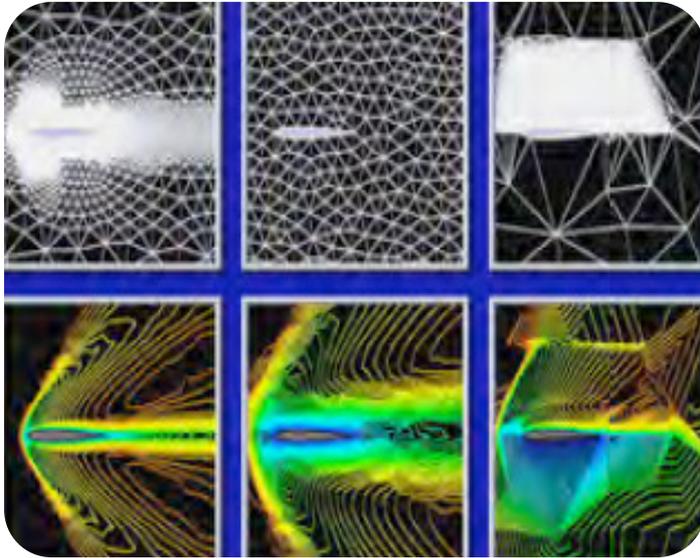
Figure 5.6   Mesh adaption
                (Habashi 2004)

5.1.6 GUI

Userfriendly GUI ensures good solution demonstration. Hence helps to assembly modules to control inputs, global values, job monitoring and result achieving. (**Figure 5.7**)
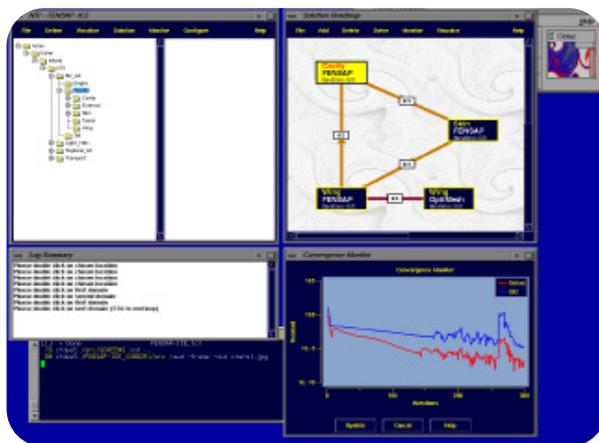
Figure 5.7   FENSAP-ICE graphical user interface
                (Habashi 2004)

5.1.7 Validation

The validation of the different modules mentioned above were done with experimental data and compared with other codes like LEWICE and 2-D test cases and 3-D geometries like helicopter parts **Figure 5.8**. The catch efficiency module DROP3D demonstrates good results in different cases with various airspeed and mass flow. Some deviations are reported at great angles of attack but with acceptable outcome.
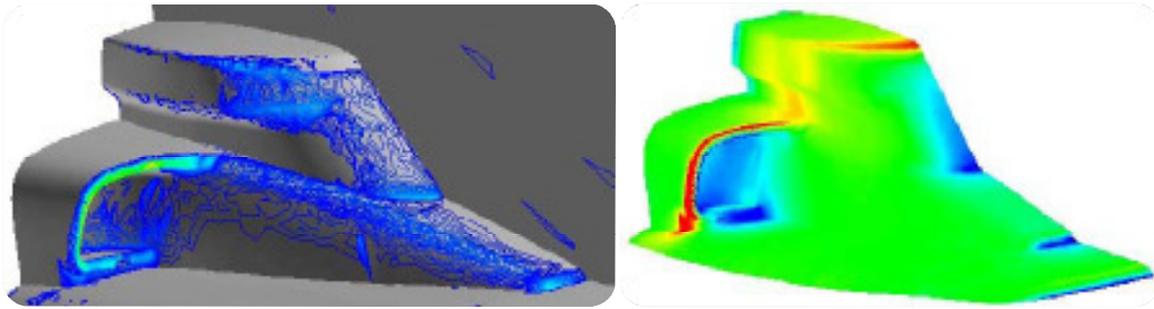
Figure 5.8   Catch efficiency distribution (left) and Mach number distribution on helicopter forward-facing inlet.
(Habashi 2004)

During computing there are possible gain of accuracy because of the flexible mesh adaption by increasing the number of nodes and tetrahedral. **Figure 5.9** shows the validation and mash adaption against a BOEING 737 engine inlet tube with experimental data from the NASA.

In summary more complex icing procedures can be regarded, without risks, reducing inaccuracies by reducing the amount of experimental test and better interworking during the design period. FENSAP shows its strength in computing complex 3-D structures for industrials research. Test and certification costs can be reduced achieving reducing test risk. Although FENSAP predict good results some effects can be simulated yet and numerical researches will be accompanied by experimental icing tunnel test. For future work the capable range off problems should be extend by improving code and implement new mathematical models. So the following points are consider to be integrated:

- SLD models
- ice shedding models
- ice particle trajectory tracking
- one-shot MVD calculations,
- droplet splashing and breakup
- **simulation of electro-thermal heater pads**
- simulation of sand
- dust, hail and rain particles
- stability and control of iced aircraft
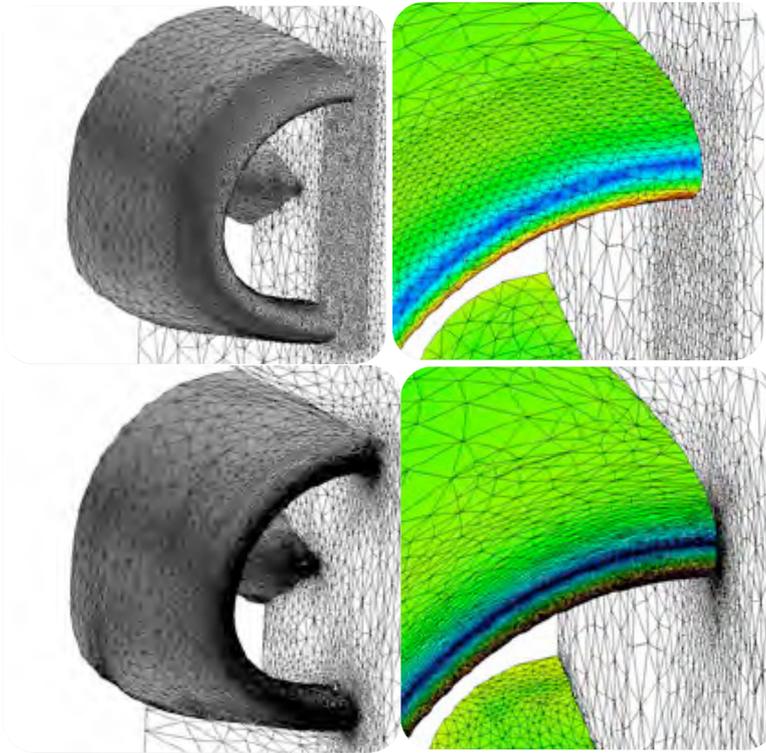
Figure 5.9 FENSAP-ICE module validation against a BOEING 737 engine inlet
(Habashi 2004)

5.2 CANISE code

The CANISE code was developed to support the efforts off the FAA and Bombardier
Aerospace in a trustworthy ice accreditation simulation certification process. CANISE uses a
potential flow solver for the airflow and the impingement droplets around an airfoil
(PARASCHIVOIU 2001) Furthermore the potential flow field is solved by an aerodynamic
panel method. To identify the trajectories of water droplets and the interaction with the airfoil
a Lagrangian estimate is used. The input data consists airfoil (altitude, angle-of attack,
airspeed) and atmospheric (temperature, pressure, water-droplet size) information. CANISE is
capable to simulate multiple layers of ice accretion by adapting the geometry and compute the
flow field around the new shaped airfoil. Simulations of flow field and ice accretions are used
to simplify the estimation a first "hot-air anti-icing model". The determination last until the
surface temperature reaches the achieved value. CANISE could be used for a wide field of
investigations listed in **Figure 5.10**.

Two additional steps are required for anti-icing simulation. An internal flow field which hot-
air jet inside the airfoil is allowed to heat up the inner surface of the airfoil leading-edge is
determined. Hence temperature distribution through the airfoil skin and the thermodynamic
balance in the boundary layer is calculated. To gain a solution an iterative procedure is

required. As a result the ice melts and water flows as runback. Until running back the water cools down and transformed back into ice away from the surface being heated. New versions of CANISE are able to use heat and mass transfer, surface temperature and accretions to compute the anti-icing energy.

Configuration		Impingement Limits	Impingement Efficiency (β)	Ice Shape Determination
Airfoil	Single Element	✓	✓	✓
	Multi Element	✓	✓	✓
Wing	Sweep > 25 deg	✓	✓	✓
	Sweep < 25 deg	✓	✓	✓
	3D, twisted			
Winglet		✓	✓	✓
Empennage	Vertical Stabilizer	✓	✓	✓
	Horizontal Stabilizer	✓	✓	✓
Canard		✓	✓	✓
Nacelle		✓	✓	✓
Pylon		✓	✓	✓

Figure 5.10   Available CANICE application
                     (PARASCHIVOIU 2001)

The simulation works as follows (**Figure 5.10** and **Figure 5.2**) .

1.   Determine the Cp distribution on the airfoil

2.   Rate of water impinging with the airfoil by following the airstream

3.   Heat balance (freezing water or evaporate/runback on the surface)

4.   Computing the ice shapes building up

+

•   Identify the internal hot air flow from the tubes inside the leading edge

•   Heating up the skin of the leading edge -> modifying the thermodynamic balance iteratively until solution was found.

5.2.1   Summary

Including new technology CANISE has a lot of room to improve results. To make CANISE more reliable and robust some of the near future improvements has to be implemented:

- Skin-friction and heat transfer coefficients based on the Kays and Crawford's relations and need to be revised based on latest experimental data on ice shapes.
- The code doesn't have a provision for SLD (Supercooled large droplets) cases. The equivalent sand-grain roughness height is being determined from an empirical relation that does not cover the SLD range.
- Relative humidity should be considered in order to better simulate the experimental conditions.
- Constant values for most of the physical properties such as density, viscosity, thermal conductivity, and latent heats are used.
- A constant value for the density of ice is currently being used

In summarizing CANISE shows good results compared to state of-the-art icing codes and experimental results in relevant cases (**Figure 5.11**). Like all other codes CANISE result doesn`t fit exactly to the experimental determined results and demonstrates the amount of work that have to be done to improve the numerical icing methods (**Figure C 4**).
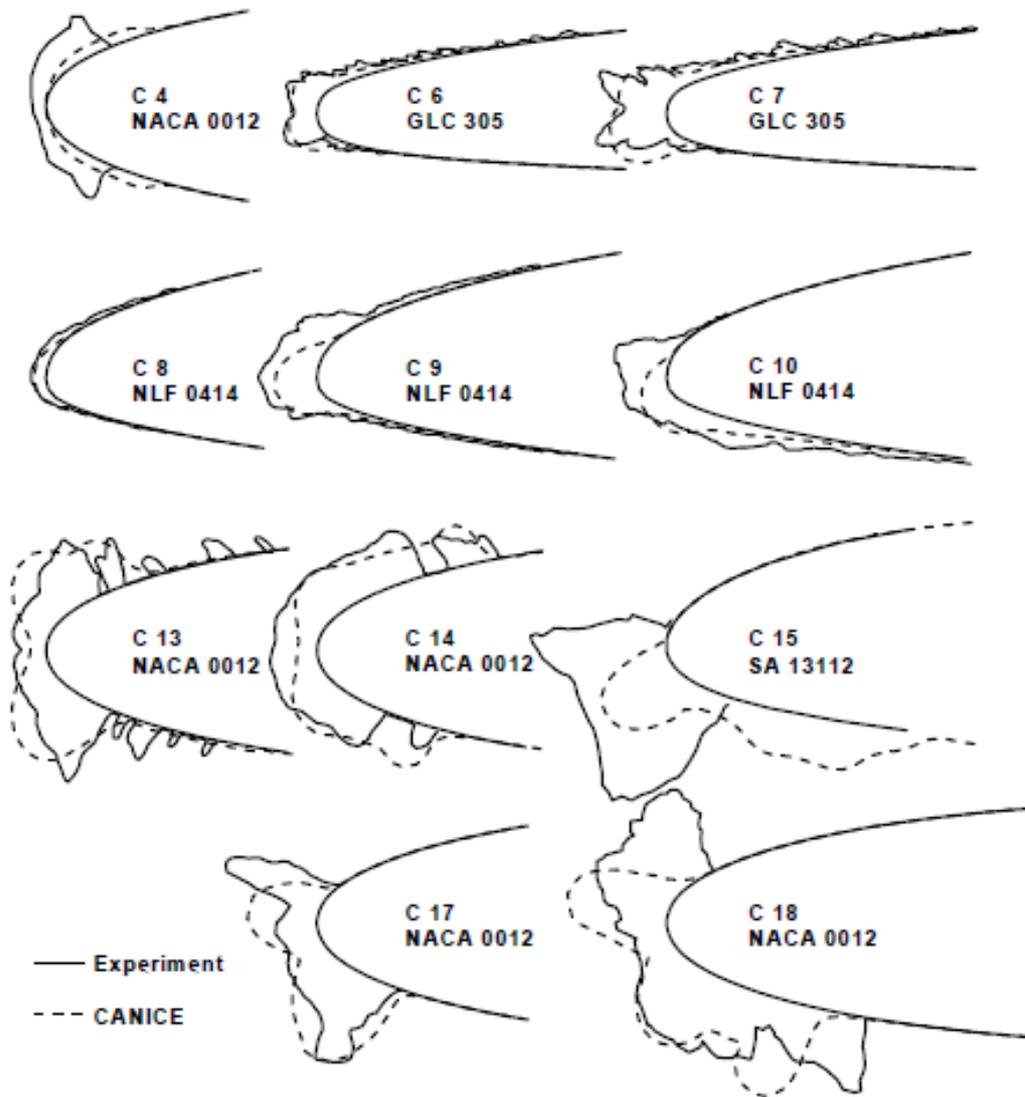
Figure 5.11   CANISE compared to icing test results
(Bragg 2002)

5.3 ONERA method

5.3.1 Brief description

The ONERA method is a 2 dimensional computer code to forecast ice accretion at 2-d airfoils. It comprises thermodynamic calculation methods which involved at developing double horns by according constraints. The program splits up into 4 different sub parts which computes the flow field, the trajectories, heat exchange coefficients and finally the ice accretion. All sub parts are written in FORTRAN 77 and work on every common computer environment. ONERA is validated for "common" airfoils and certified as aid of airplanes from the JAR. The method isn't generally available and has to be requested from the ONERA. (**LTH 2008**)

5.3.2 Flow field

Background is the potential equation which approximately solved with the finite-difference-method. A C-net is used to have e better control of the wake (**Figure 5.12**). Furthermore on the one hand the influence of the mach number is considered but leaving out the factor of the boundary layer. (**LTH 2008**)
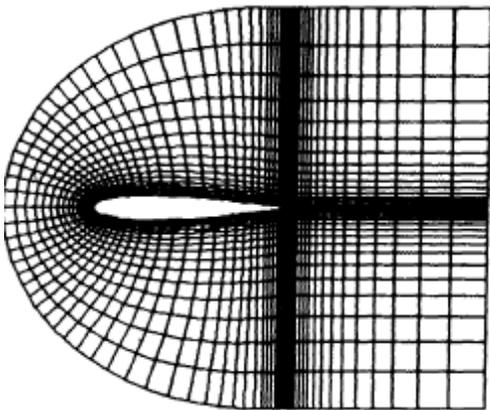
Figure 5.12   C-net with good resolution at the end
                    (Gehrer 1999)

5.3.3 Trajectories

The trajectories of the droplets are computed by integration of the equation of motion. In the beginning the upper and lower boundary trajectory are determined by an iterative process. Finally the LWC yield observing two adjacent trajectories. (**LTH 2008**)

5.3.4 Heat exchange coefficient

For the upper and under side of the airfoil the boundary layer is computed for laminar and turbulent flow outgoing from the point of stagnation to get the local heat exchange coefficient. The factor of roughness is replaces by an equivalent factor. (**LTH 2008**)

5.3.5 Ice accretion

Ice accretion is simulated for each surface element by using the energy- and mass balance. Outgoing from the point of stagnation each side is considered separately. Runback is added to the next following surface element to fulfill the mass balance. (**LTH 2008**)

5.3.6 Program input

The following files have to be created to ensure a correct program flow.

PROF.DAT: This file contains the formatted coordinates of the airfoil shape. Only the upper side has to been in the front and the underside in the backward. (**LTH 2008**)

CCHAMP.DAT: This file contents for example mach number and angle of attack which are necessary to solve the flow equation. At adding commands at NAMELIST-Form every setting at the main program can be reseted or changed. Here an overlap of mesh lines and other inconsistence can be prevented which throws an error "STOP 2000" and terminates the program. (**LTH 2008**)

DTRA.DAT: This input file is necessary to compute the heat exchange coefficient and trajectories. It contents environmental variables like pressure, mach number, temperature, droplet diameter and number of trajectories. (**LTH 2008**)

DCAPT.DAT: Here icing input parameters are defined like water content, freezing time and a time table for the second run (KCAL = 1). (**LTH 2008**)

5.3.7 Program sequence

The different sub parts (flow field = POTFLOW, trajectories = TRAJEC, heat exchange coefficient = ALPHACP, ice accretion = SHAPE) have to run twice (**Figure 5.13**). The first time a temporary ice accretion is computed and with the second run the final accretion is determined. Is KCAL set to 0 the second run will set it to 1, terminate the program and will show the result. The sequence has to been run in the right order due to the following sub parts depend on the results from his precursor. The program sequence looks like the flow chart below:
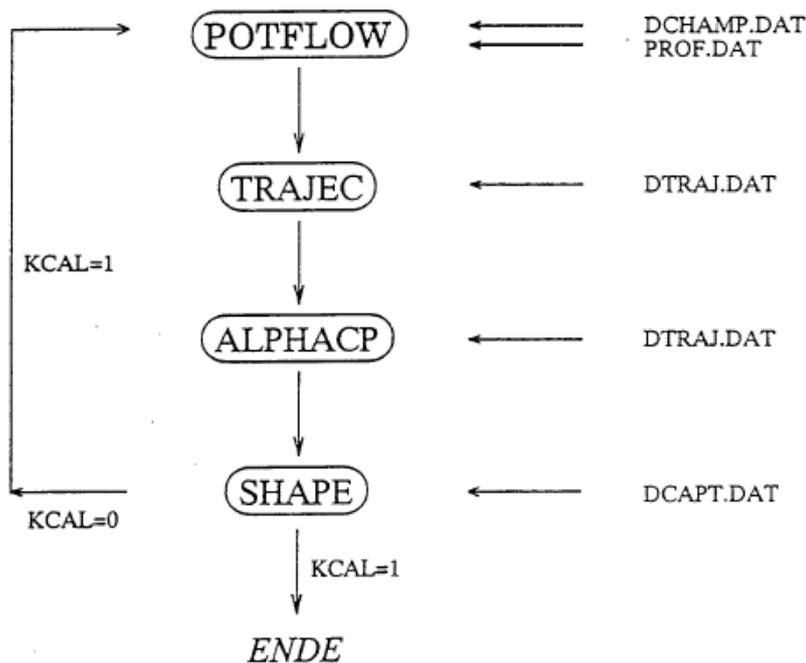
Figure 5.13   ONERA program sequence
                        (LTH 2008)

5.3.8   Program Output

Every sub part of the program creates its own result file which can be interpreted separately by plotting the results (**Figure 5.15**). Furthermore the mesh can be checked, the trajectories, the LWC can be plotted and the ice accretion can be shown by comparison with the origin airfoil shape. (**LTH 2008**)

5.3.9   Validation

The ONERA method was validated by measurement data from NASA (Lewis icing channel test with NACA 0012). **Figure 5.14** shows measurements at different temperatures. Yield that the experimental data fit well with the ONERA computed accretions for rime and glace ice. The quality depends among other thinks from the mesh quality and trajectories density. ONERA is certified by FAR and JAR for aid at aircraft certification but doesn't replace natural icing flight.

The method is used if a "normal" airfoil exists and covers the range from general aviation, commuter airplanes and commercial aircraft:

- thickness between 8% and 18%
- chamber between 0% and 5%
- position of maximum thickness/chamber 25% ~ 50%
- mach number Ma~0.5
- chord between 0.5m and 2.5m

NACA 0012 $c = 0.53$ m ; v_∞ = 209 km/h ; $\alpha = 4°$; LWC = 1.3 g/m³ ; MVD = 20 μm ; Δt = 8 Min.

$T_{tot} = -26°C$

$T_{tot} = -18°C$

$T_{tot} = -12°C$

$T_{tot} = -5°C$

$T_{tot} = -2°C$

$T_{tot} = -1°C$

——— Rechnung
- - - Messung
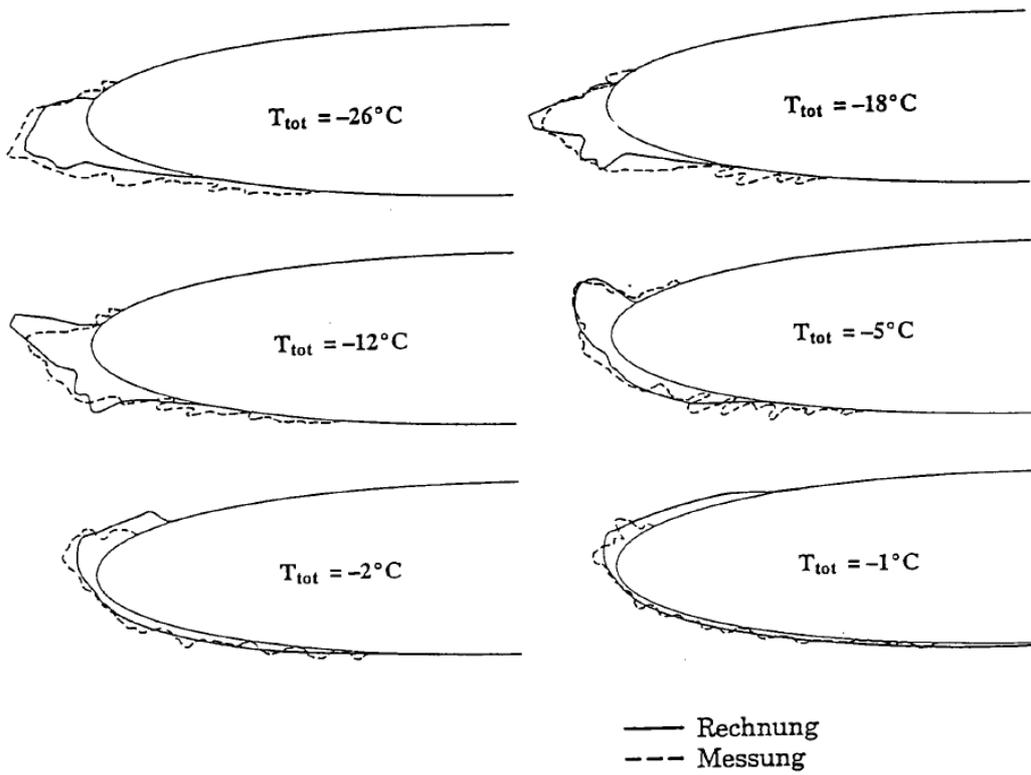
Figure 5.14   Comparison ONERA and experimental data
(LTH 2008)
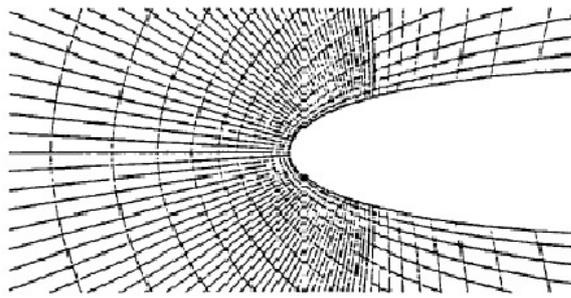
Netz KCAL=0
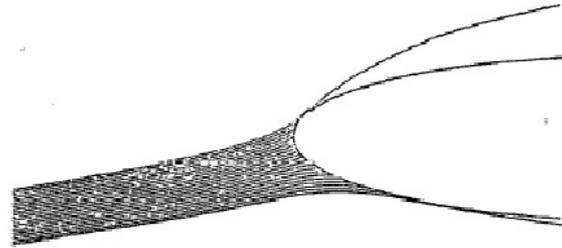
Trajektorien KCAL=0
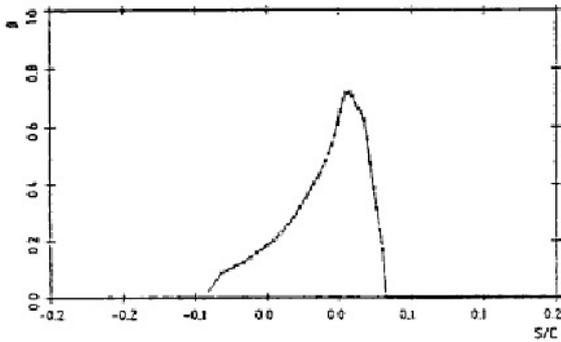
Wassereinfangrate KCAL=0
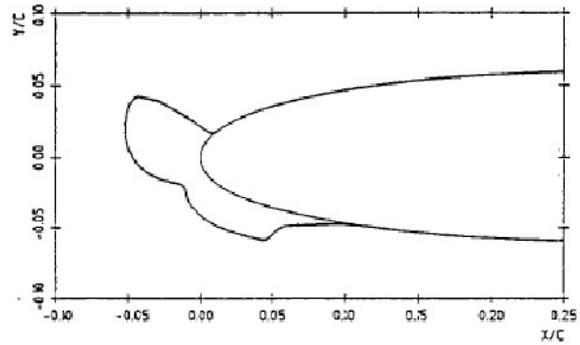
Vorläufiger Eisaufbau KCAL=0
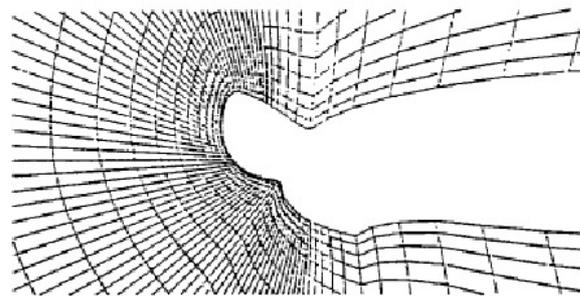
Netz KCAL=1
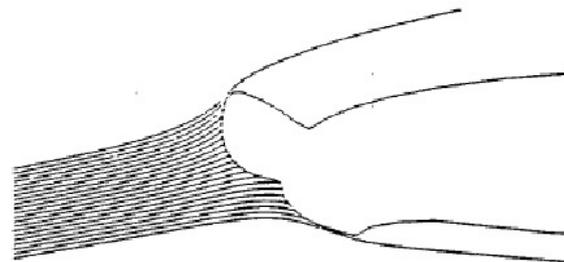
Trajektorien KCAL=1
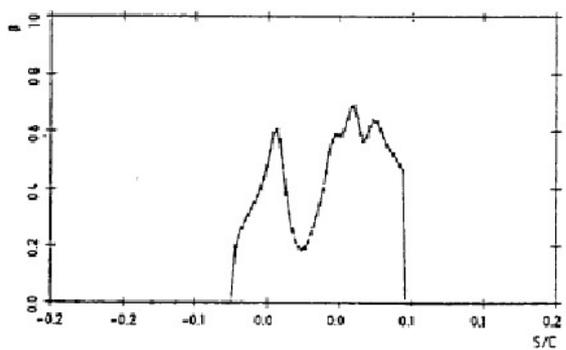
Wassereinfangrate KCAL=1
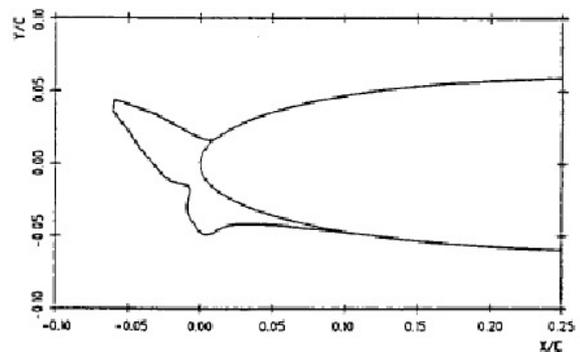
Endgültiger Eisaufbau KCAL=1

Figure 5.15 **P**lot of the sub part results
(LTH 2008)

5.4   LEWICE code

During the nineties of the 20th century the NASA and their industrial partners consider the need a computer code for thermal ice protection computer code. So during the following years two codes [LEWICE/Thermal (electrothermal de-icing and antiicing) and ANTICE - (hot gas and electrothermal antiicing] were developed and validated against experimental data.

Two airfoils were prepared one with electrothermal ice protection system to validate the de-/antiicing modules of LEWICE/Thermal and ANTICE and the second with hot air antiicng system to compare the results with the hot air anti-ice module of ANTICE. LEWICE/Thermal compute the results with the two dimensional potential flow around the airfoil together with:

- calculates water droplet
- impingement limits,
- water collection efficiency
- external heat transfer coefficient

which results slips into a mass and energy balance to determine the growing accretions. For future upgrades LEWICE Thermal version 1.6 and higher is more flexible and can used in ther icing codes (e.g. a grid-based Naviér-Stokes flow solver). (**Wright 1997**)

5.4.1   Code structure

The **MAIN.F** program operates the subparts of the program (**Figure 5.16**). So **FLOW.F** makes the basic model available (here the Hess-Smith potential flow code). **VEDGE.F** determines compressible effects and computes the stagnation point. The results are delivered to **TRAJ.F** which calculates droplet trajectories and the body's collection efficiency. Furthermore **BDY.F** considers the effect of boundary layer during the external heat transfer coefficient calculation. The next module **ICE.F** set the energy and mass balance formula on surface and computes ice growth rate. Finally **GEOM.F** designs a new geometry (airfoil + ice). (**Wright 1997**)
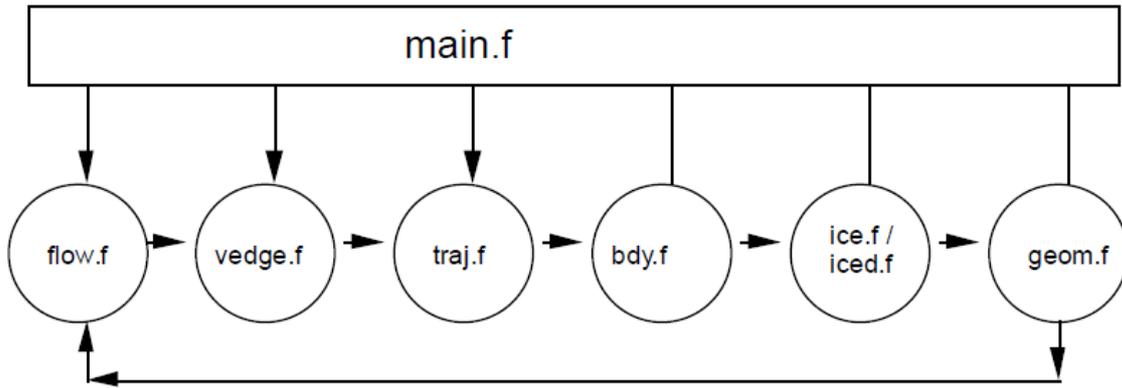
Figure 5.16   Flow chart of LEWICE 1.6
                    (**Wright 1997**)

5.4.2   Thermal Deicer Module

The module is able to compute the heat transfer in a composite structure. Furthermore it allows determining different heater layout with parted heated and cyclic energized areas. It also considers ice growth, ice shedding and water runback. During development following functions has been integrated:

1.   Thermal module is fully integrated into the process and is able to run cyclic energized areas.
2.   Support cyclic de-icing with computing the ice accretions even when the surface is unheated or during turn off times.
3.   Advanced runback model and improved energy balance.
4.   Regarded ice shedding by comparing the adhesion force and aero forces to decide whether the ice will shed or not.
5.   More complex cases have been implemented making the computing more robust.
6.   Tracing the shed ice particles with the particle trajectory code.
7.   Heater on time before starting the icing procedure
8.   Individually heater layout with different areas, temperature range and on/off time to depict real system layouts.
9.   Simulates heater materials where the thermal resistance is a function of temperature to meet the industries needs.
10.   Heater layout don't depends on the shape and design of the system (heated slat while other elements are unprotected)
11.   Heater can compute with an offset to solve integration and production issues.
12.   All units are metric for better compatibility
13.   Contour plots are integrated for better detailed output.

14. "Fast solution" for approximation and first steps toward pre-dimensioning
15. More than one data style is created at a time to view different aspects of one run.

5.4.3   Results

For the experimental test and validation a NACA0012 airfoil was used. The heater layout distinguishes seven heated areas which can be controlled individually and are integrated into the composite structure. (**Wright 1997**)
The test matrix consists of two general parameters:

1. Icing parameters (T, LWC, MVD etc)
2. Electrothermal parameters (on/off time, power input)

Four basic conditions were chosen for the icing test:

Table 5.2   Basic conditions
according to **Wright 1997**

Condition	T_0 [F°]	V [mph]	LWC $[\frac{g}{m^3}]$	MVD [µm]	Htr.A $[\frac{W}{inch^2}]$	Htr.B,C $[\frac{W}{inch^2}]$	HtrD-G $[\frac{W}{inch^2}]$
1	20	100	0.78	20	5	10	8
2	20	100	0.78	20	5	7	7
3	0	100	0.78	20	10	12	10
4	0	100	0.78	20	12	16	15

The cyclic heating with an off phase of 110 sec. and a heating phase with 10 sec. has been occurred as best during the experimental tests where the heat flux and the cyclic time are the most important parameters. The energy per heater for the first case was set to: (**Table 5.2**)

- Heater A: $5 \ \frac{W}{inch^2}$ [parting strip]

- Heater B,C: $10 \ \frac{W}{inch^2}$

- Heater D-G: $8 \ \frac{W}{inch^2}$
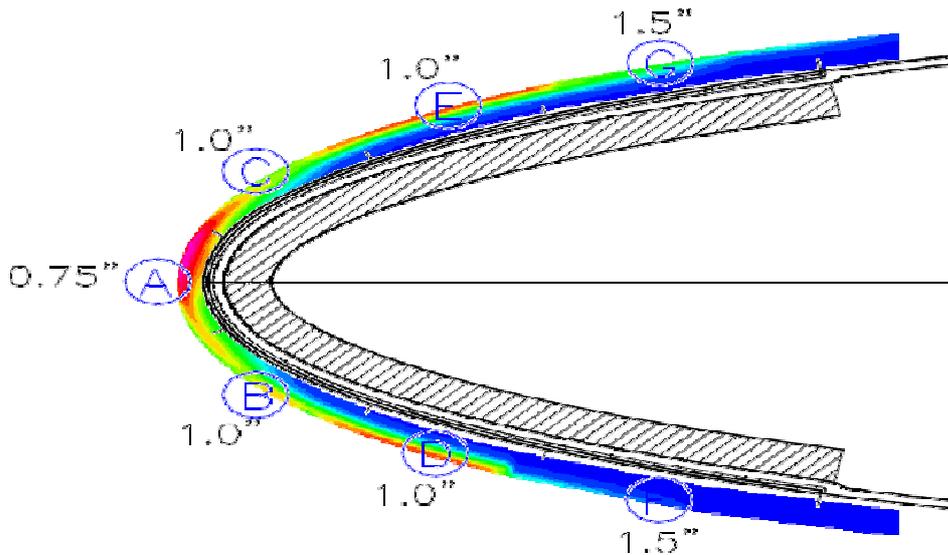
Figure 5.17   Shows the temperature contours in the airfoil at a particular time (not the first case)
                    (Wright 1997)

Figure 5.17 shows the leading edge temperature distribution during cyclic de-icing sequence.
Heater D to G were heated at this moment showing a greater temperature gradient and B to C
were about to turn off. Here the conductivity is obvious and are better shown than in **Figure
5.18.**
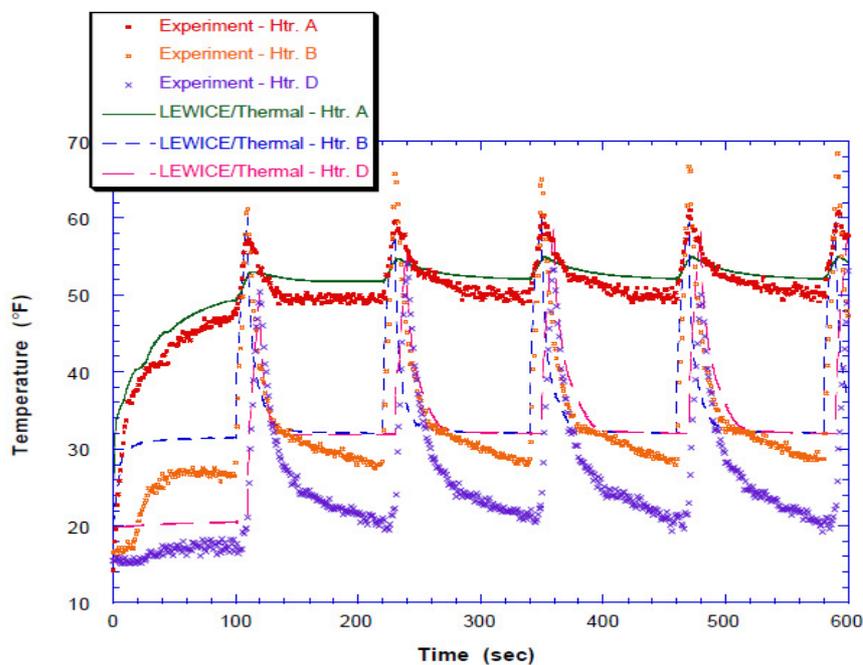
Figure 5.18   Comparison of Heater Temperatures for Case 1
                    (Wright 1997)

Figure 5.18 shows the determined heater temperature compared to the numerical value competed by LEWCIE/Thermal. The flow of surface water has a cooling effect which explains why the experimental data shows heater A cooling to its previous level after heaters B and C turn off. This occurs due to the code doesn't difference between shed ice and runback water yet.

The validation takes place at the NASA Lewis Icing Research Tunnel and shows the good performance for ice prediction. Deviations could be explained by the measure points during experimental test and predictions toward the heat exchange in composite structures. There are still problems at lower temperatures like case 3 or 4 when the icing code shows a higher temperature (Heater A) than the experimental results (**Figure 5.19).** This Problem should be solved by improving the physical model and compute the ice shed/ runback water separately and will be fixed until the code is released.
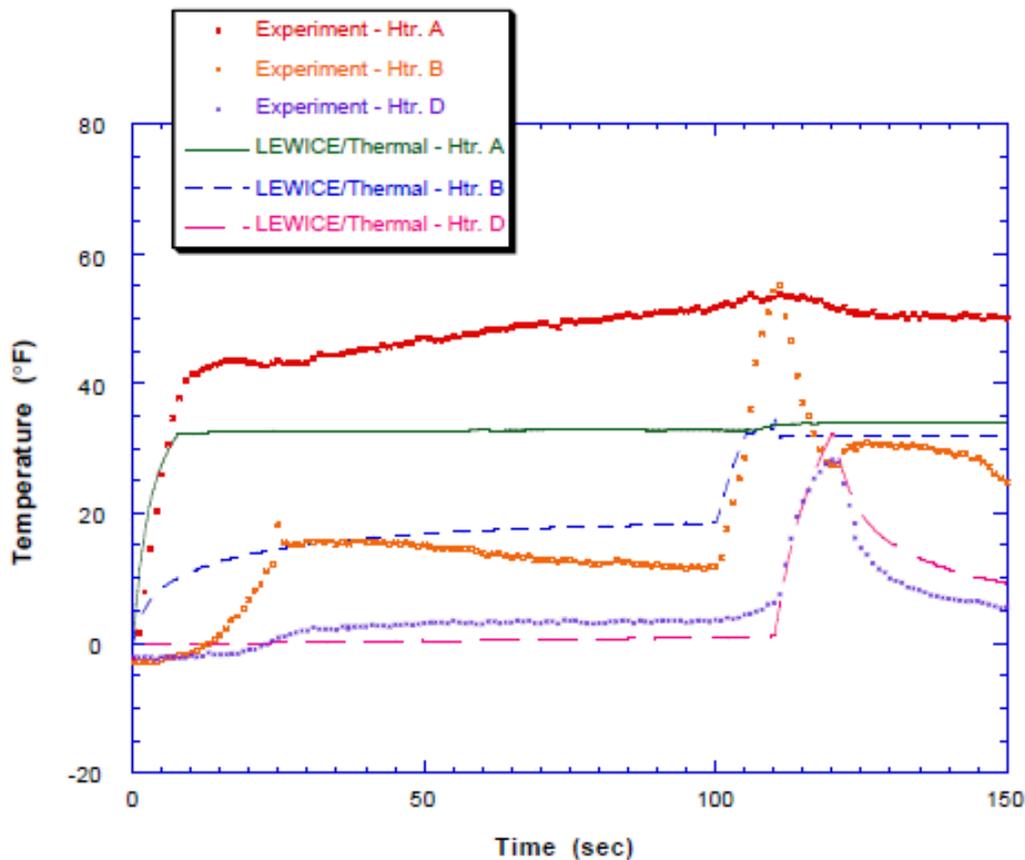
Figure 5.19   Comparison of Heater Temperatures for Case 3
(Wright 1997)

5.5   Summary of the CFD codes

The CFD methods introduced above show the today's potentials in computing icing conditions and determine the accretions and energy needed to de-ice areas during those conditions. **Figure 5.20** show that there are already some icing programs which are able to predict icing conditions with different variable conditions and airfoil shapes. The results demonstrate that a 100% prediction isn't possible but a good approach can be accomplished. Some different codes have problems with the rime ice accretion due to neglecting microphysical factors and bead formation.

In summary icing codes enables computational rime ice and glaze ice accretion prediction on single and multi-element airfoils in acceptable time of solution. The mathematical models have recently been modified for better results and to compute for example variable wall temperature along the airfoil surface. The programs were also improved for the better approximation of transition boundary layer location. The simulation of ice formation presents many challenges due to the phenomenon explained are highly chaotic so the result of an experiment does not give identical ice shapes. The important reasons why computed results are different from the experimental one are:

- The unpredictable behavior of water on the airfoil surface. The changing paths of rivulets are highly unpredictable. This directly affects the resulting ice shape.

- When ice starts accumulating, the resulting surface roughness varies significantly from one case to another and from the location on the surface. This is also very difficult to predict. Roughness has a great influence on the heat transfer between the water and the airflow. The final ice shape is therefore very sensitive to the evolution of local surface roughness.

- It has shown from wind tunnel testing that ice density may experience important variations for different cases. The ice density is affected by the amount of air trapped in the ice.

- The physical model used in current ice accretion codes need to be improving, especially if it is also to be used for three-dimensional flows.

C-9 NLF0414-611 Comparison Plot
Airspeed: 92.54 m/s, Stat. Temp.: 257.6°K, LWC: 0.33 g/m³,
VMD: 20.0 μm, Duration: 1224.0 secs, Chord: 0.9144 m

C-13 INTA/NASA Scaling Tests-533 Comparison Plot
Airspeed: 67.0 m/s, Stat. Temp.: 264.4°K, LWC: 0.65 g/m³,
VMD: 40.0 μm, Duration: 672.0 secs, Chord: 0.533 m

C-6 GLC305-836-22 Comparison Plot
Airspeed: 69.87 m/s, Stat. Temp.: 257.43°K, LWC: 1.16 g/m³,
VMD: 50.0 μm, Duration: 258.6 secs, Chord: 0.9144 m

Figure 5.20   Experimental results compared to different icing codes
(BRAGG 2002)

6 Icing process

6.1 Icing clouds

In Stratiform clouds and cumuliform clouds icing conditions can be predicted. As it can seen in **Figure 6.1**different cloud types occur in various altitudes.
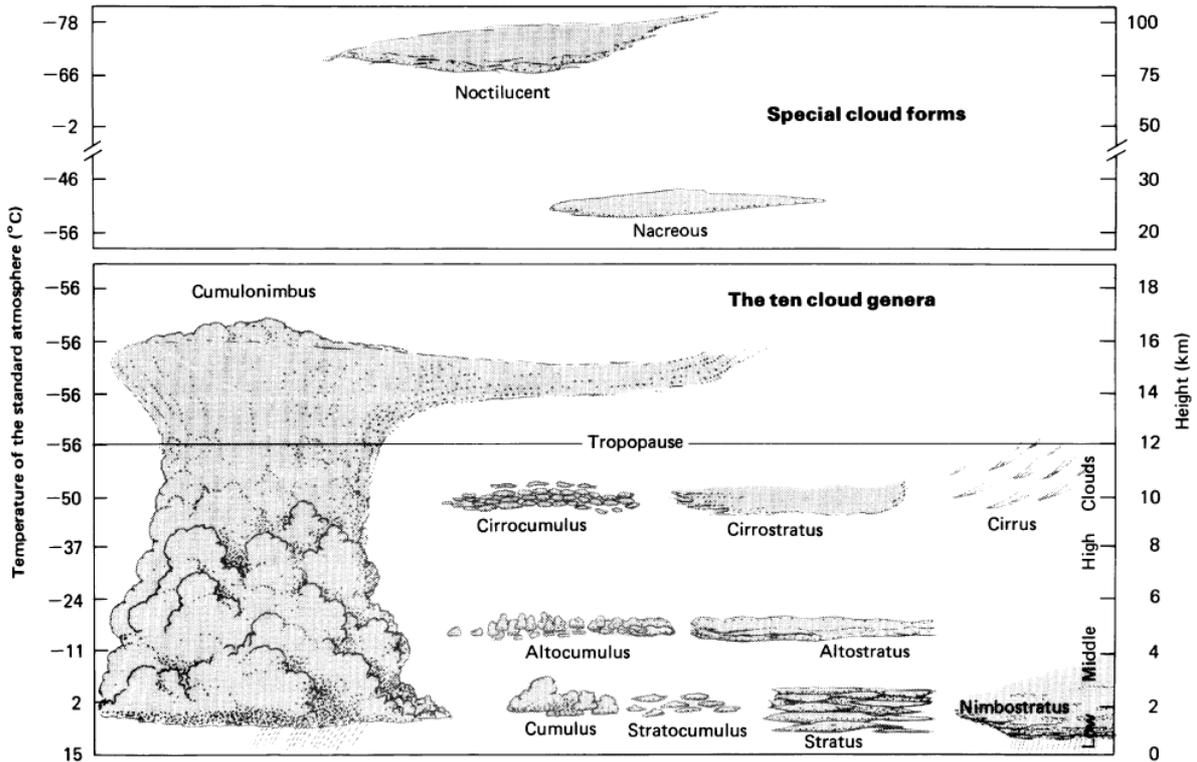
Figure 6.1   Cloud distribution and classification
             (Bragg 2002)

6.1.1 Stratiform Clouds (horizontal deployment)

Stratiform clouds show moderate icing conditions due to persistent contend of LWC from 0.1 to 0.8 g/m³ and droplet diameter from 5 to 50 μm. (Bragg 2002) However due to their much larger horizontal extension the harmful icing conditions are persistent and can't be ignored. Rime ice is the most common icing form in stratiform clouds. (Bragg 2002) They can be classified of high, middle and low level clouds (**Figure 6.2**).

At high regions above 20,000 ft only ice crystals encounters which doesn't stick to the aircrafts surface on impact. With decreasing high the icing problematic rises due to emerge of

(supercooled) water droplets (**Table 6.1**). At altitude below 6,500 ft the risk of icing is very high notably if stratiform clouds occur together with cumuliform clouds. The suggestion to evade stratiform icing conditions is to fly at lower altitude where the temperature is above freezing or climb up where only ice crystals exists. The FAA denotes conditions at this genus of clouds as documented in envelope of the **Appendix C** part 25 (**see Fig. 1 and following**).

Cloud Type ⇒ Precipitation ⇓	AS Middle clouds (2 to 7 km)	NB	SC Low clouds (below 2 km)	ST	CU	CB Vertical development
Rain	✓	✓	✓		✓	✓
Drizzle				✓		
Freezing drizzle			✓			
Snow	✓	✓	✓			✓
Snow pellets			✓			
Ice pellets	✓	✓				✓
Ice prisms				✓		
Hail						✓

Figure 6.2   Precipitation as a function of cloud types
                        (Bragg 2002)

Table 6.1   Characteristics of low clouds, below 2 km (6,500 ft).
                        (according to **Bragg 2002**)

Cloud type	Composition	Appearance
Stratocumulus (SC)	Water droplets (rarely some ice crystals)	Soft gray clouds in the form of large globules patches. May resemble puffs of cotton. When overcast, they produce an irregular pattern of light and dark patches larger than AC.
Nimbostratus (NB)	Mixture of ice crystals and water snowflakes ordroplets, raindrops near base	Gray or dark layer with no distinct cloud element. Thick enough to obscure the sun. Produces precipitation and may be obscured by lower stratus clouds.
Stratus (ST)	Water droplets (rarely some ice crystals)	Low uniform layer resembling for but not resting on the ground. Sun and moon are not visible through it except when layer is very thin.

6.1.2 Cumuliform Clouds (Vertical Development)

In contrast to the stratiform clouds Cumuliform Clouds have a much greater LWC from 0.1 to 3.0 g/m³ and may reach 3.9 g/m³. Due to turbulences and massive exchange of vertical air mass which may support supercooled droplets, glaze ice accretions my build up in less time. Due to the vertical development in cumuliform clouds intermittent icing appears (**Figure 6.4, Table 6.2**).

Table 6.2 Characteristics of clouds of vertical developments.
(according to **Bragg 2002**)

Cloud type		Composition	Appearance
Cumulus	(CU)	Water droplets	Detached dense vertically developed clouds often characterized by flat bases. Horizontal base is usually dark.
Cumulonimbus	(CB)	Mixture of ice crystals and water droplets	White dense clouds with great vertical development, associate with heavy rainfall, thunder, hail and tornados.

6.2 Design Point

Certification requirements for flight in icing conditions are stated in CS 25.1419 of CS-252008. The aeroplane must be able to safely operate in continuous maximum and intermittent maximum icing conditions as defined in CS-25 Book 1 **Appendix C**. In order to verify this, an analysis must be performed followed either by laboratory dry air simulated icing tests or by flight tests. The first regulations and considerations about icing conditions has been done by the National Advisory Committee for Aeronautics (NACA) and later adapted by the Federal Aviation Administration (FAA). An attempt to simulate and describe regulations of natural icing flights for jet and transport aircraft. Two circumstances (continuous and intermittent maximum atmospheric icing) are linked to describe atmospheric conditions. **Figure 6.3** and **Figure 6.4** show icing conditions of two different cloud types (Continuous maximum = stratiform clouds, Intermittent maximum = cumuliform clouds). Important parameters are LWC, droplet diameter, ambient temperature, altitude, horizontal extend and the types of cloud. The abscissa represents the mean droplet diameter and is torn down over the LWC.

Continuous icing conditions regarded for altitude between sea level and 22,000 ft by typically droplet diameter around 20 µm. The temperature depends on which protections system is used. Due to the cloud formation and continue characteristics the vertical extent is set to 6,500 ft and horizontal standard distance is 20 miles (**Figure 6.3**).
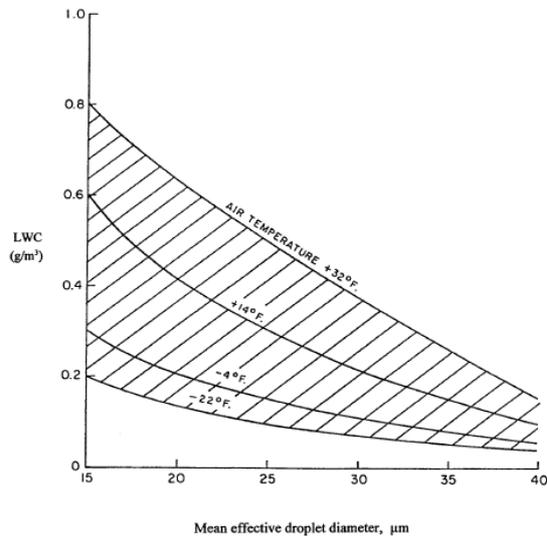
Figure 6.3   Continuous maximum atmospheric icing conditions for stratiform clouds, FAR 25 Appendix C (horizontal extent 20 miles).
(EASA 2008)

Intermittent icing conditions describe horizontal extends distances for 3 miles. The clouds contend high LWC which can be seen by **Figure 6.4** and the temperature extends to -40 °C. At even lower temperature or altitudes above 24,000 ft icing conditions are exceptional. Those conditions are used for engine inlets which are exposed to a high LWC.
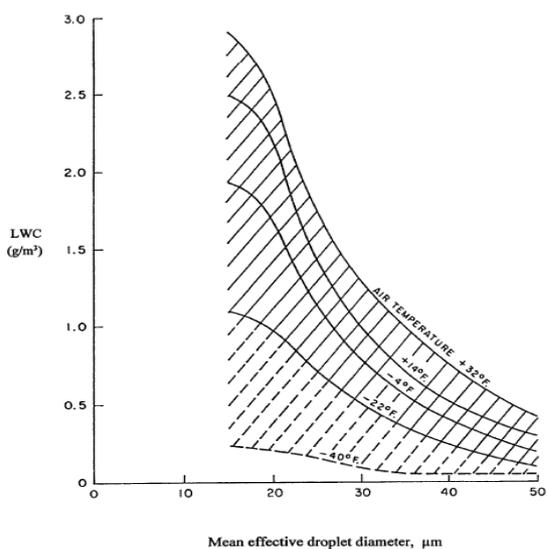
Figure 6.4   Intermittent maximum atmospheric icing conditions for cumuliform clouds, FAR 25 Appendix C (horizontal extent 3 miles).
(EASA 2008)

The intent of different icing conditions in FAR 25 is to cover extreme icing conditions in order to design the ice protection systems. The FAA icing criteria is being reviewed and regulation are discussed based on the modern cloud observations, particularly for supercooled large droplets exceeding the maximum value of droplet diameter presented.

6.3   Ice types

Many different types of ice types exist in the atmosphere. Solid forms like hail, ice crystals, and snow doesn't adhere well to cold surfaces like leading edges or other critical structures of the aircraft.

Drizzle or mist is numerous water droplets or ice crystals in the air. With a high humidity and water drops with diameters less than 0.5 millimeters. It's formed by the cooling of land after the sunset or air passes over cool surface. Normally a reduced visibility less than 1 km is reported.

Ice crystals are small ice crystals including many various forms. Cause of their very small size and weight they are suspended in the air and causes many optics displays.
Snow is composed of small ice particles and snowflakes and fall through the atmosphere in form of a ball due to melting effects.

Hail is precipitation in the form of solid ice stones. There diameter varies between 5, 50 mm and more. Hail is layered and consists of clear ice and dull layers. Mostly the weather phenomenon comes along with high wind speeds and thunderstorms. More hazardous are super cooled liquid precipitation or condensate icing. These forms are able to form ice accretions especially at the wings and other exposed aircraft structures. **(Majed 2006)**

6.3.1   Rime ice (dry ice growth)

Rime is white ice that forms from small supercooled water droplets which freeze on impact. Due to the lower temperature water droplets freeze rapidly before the drops have time to spread over the surface **(Majed 2006)**. This type of ice accretions builds up on exposed parts of the aircraft. The small droplets freeze nearly instantly completely and capture little air bubbles during the process which gives an opaque occurrence. Hence a liquid layer on the surface is created and hardly runback remains thus less disruption in the airflow and lower

performance problems. This process is called the dry ice growth. Rime ice is fragile and easier to remove than glaze ice (**Figure 6.5**)
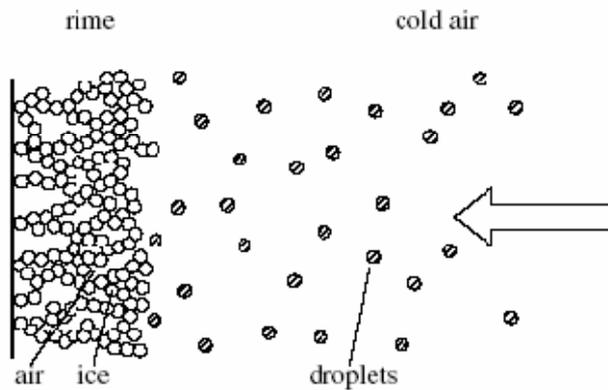
Figure 6.5   Rime ice
                     (Majed 2006)

Rime ice is mostly come across in Nimbostratus clouds and also in radiation fog at negative temperature in high pressure area at temperature -20 °C and below.

6.3.2   Clear ice (wet growth ice)

Clear ice or **Glaze** ice is formed from large supercooled fog droplets when they strike over a surface at temperatures at or below frost point. It exits in clouds with high liquid water content and temperatures from 0 °C to -10 °C. During the formation and the slow freezing process the water droplets don't freeze completely and the excess water runs off at the surface and builds up horns or other shapes. The slower the freezing process, the greater the flow-back of the water before it freezes **(Majed 2006).** During the process no bubbles are captured giving the ice a clear and transparent aspect. Glaze ice is denser, harder and more transparent than rime ice (**Figure 6.6**)
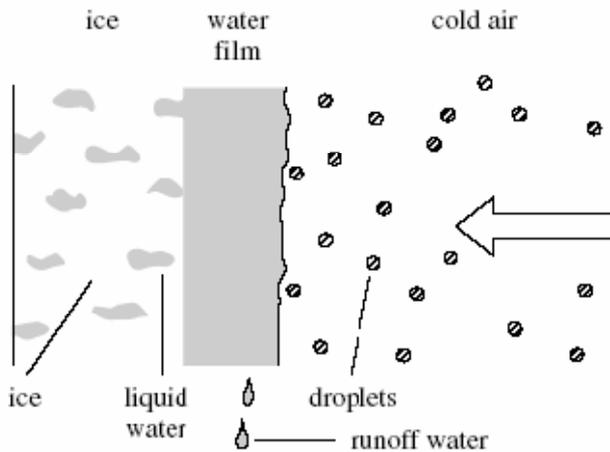
Figure 6.6   Glaze ice
                    (Majed 2006)

Due to his high density it makes it difficult to remove it. Clear ice forms in cloud layers with high liquid water contend large droplet size and slow drainage of the latent heat of fusion. Due to the mixed content and droplet size in a cloud glaze ice and rime ice occur simultaneously as mixed ice. **(Bigarré 2003)**

6.4   Icing principles

Shape and characteristics of ice accretion depends on temperatures just like the ice types. Below and above -15 °C there is a different behavior of supercooled droplets since they strike the leading edge of the wing. Above -15°C only a small part of the supercooled water (freezing fraction) freeze directly at point A forming a concave hollow. Hence the remaining supercooled water runs back freezes between point B and C forming lobes. Result will be glaze ice at this temperature and above (**Figure 6.7**).
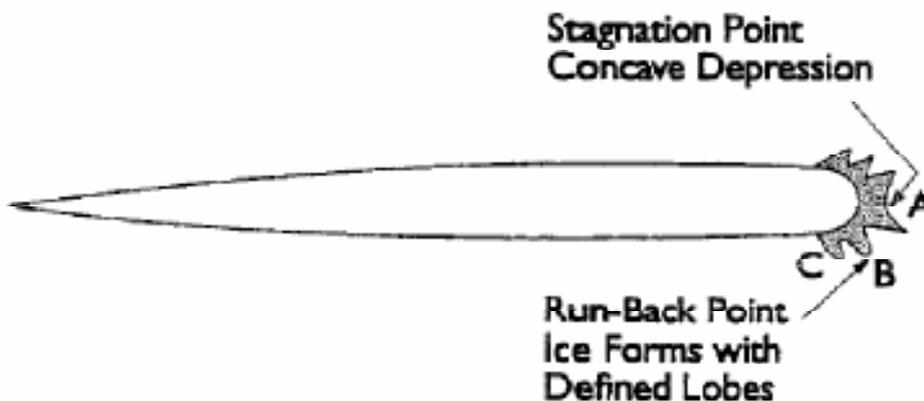
Figure 6.7   Leading edge ice formations at temperature above -15 Co
                    (Majed 2006)

Below -15 C$^{\circ}$ ice forms build up in a symmetric form on the leading edge at the stagnation point. By comparison with much higher temperatures like in **Figure 6.8** the freezing fraction is much higher and causes less runback water. Hence the development of rime ice will be promoted.
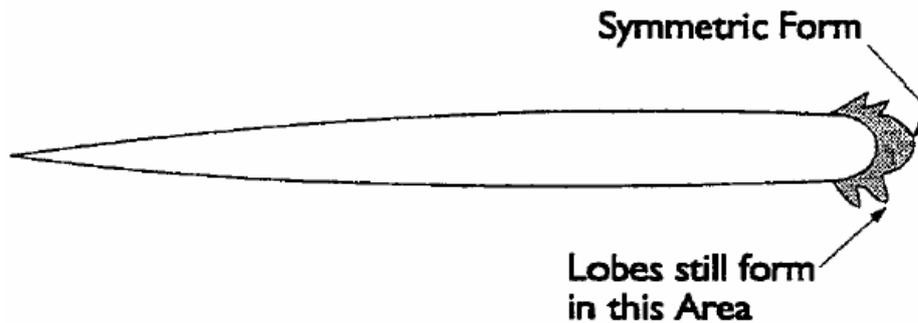
Figure 6.8   Leading edge ice formations at temperature below -15 Co
(Majed 2006)

6.4.1   Liquid water content – LWC

Table 6.3   Standard water contend according to **Bigarré 2003**

Medium	Water content g/m³
Fog	0.1to 2
Stable clouds	0.2to 0.5
Unstable clouds	1 to 3

The water content isn't a uniform value but for standard conditions some assumptions for better calculations can be assume (**Table 6.3**). LWC depends on the temperature and is essential for the approximation for icing forecasts. Hence the distribution of supercooled water droplets depends on the high above mean sea level and the atmospheric layer (**Figure 6.9**). Furthermore with rising elevation more and more water droplets freeze completely and supercooled water droplets disappears below -40 °C.
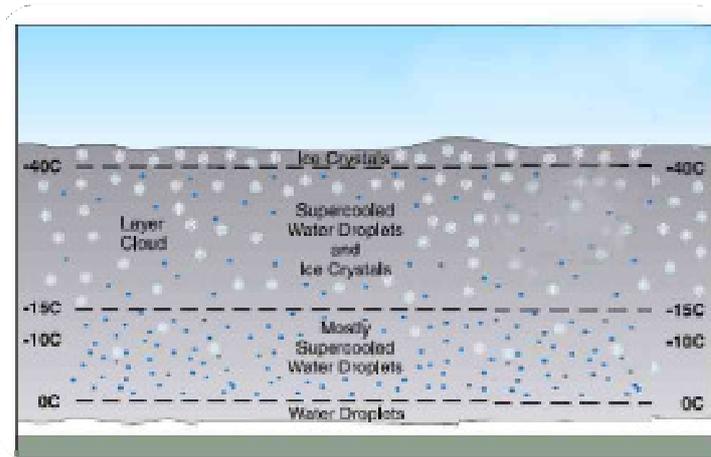
Figure 6.9 Liquid water content varies with temperature
(Majed 2006)

6.4.2 Airfoil Shape

Shape and airfoil thickness influences the air flow in different ways and causes various characteristics at icing conditions. Increasing the leading edge radius yields a reduced ice accretion due to deeper boundary layer. Much smaller droplets are centrifuged off and carried around the airfoil without striking it. Hence the icing effect is reduced. On this account, thin super critical high speed airfoils collect ice more efficiency than large thick airfoils (**Figure 6.10**)
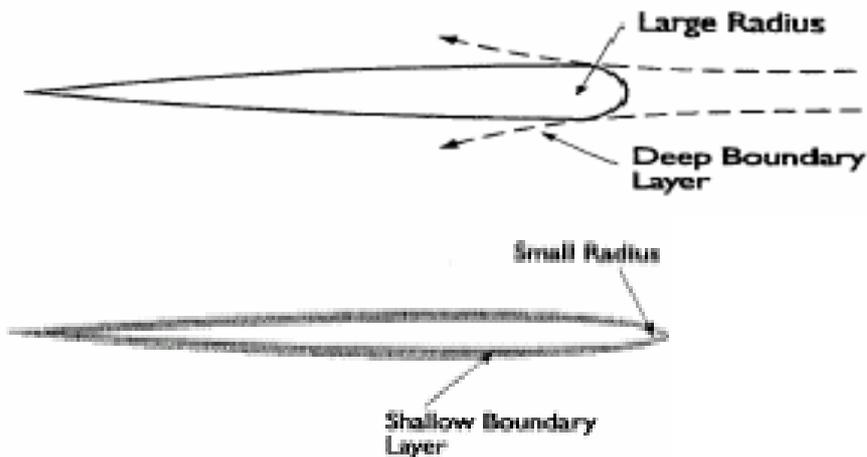
Figure 6.10 Leading Edge Radius
(Majed 2006)

6.4.3   Velocity of air stream

The higher the air velocity the lower is the chance that the droplets are deflected and follows the shape of the airfoil (**Figure 6.10**). Hence at higher velocities more droplets collide with the surface. This rule only applies to certain limits and depends on the airfoil shape. It can be observed that at very higher airspeed the ice accretion is lowered again. (**Figure 6.11**)

Figure 6.11   Speed have an effect on ice accretion
                (La Burthe 2010)

6.4.4   Droplet size

With enhancing droplet size the weight and inertia increasing too. The airstream isn't able to divert the droplets anymore and the catch efficiency rises. Finally the water hits the surface and leads to as is well known accretions. (**Figure 6.12**)
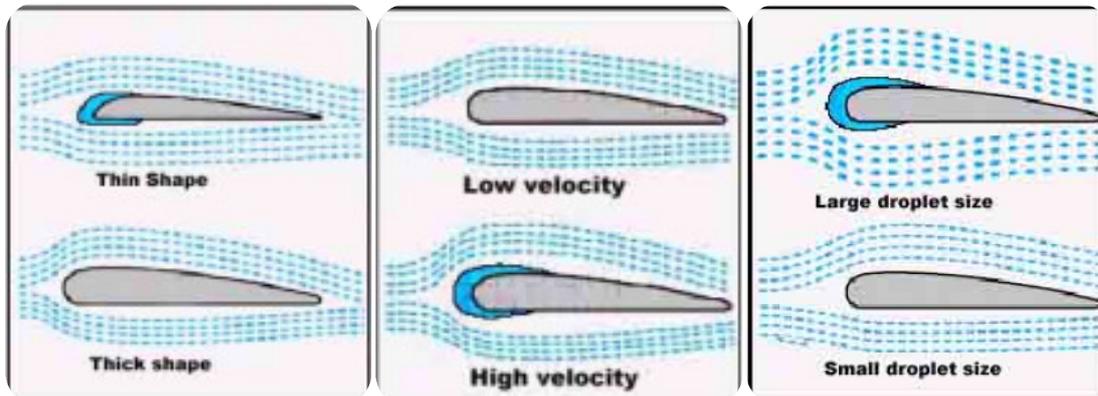
Figure 6.12   Collection efficiency as function of 1.) leading edge radius, 2.) airstream velocity
                3.) droplet size
                (Majed 2006)

6.5   In flight icing process

6.5.1   Rime ice

At cold temperature impinging droplets form bunches of (*rime*) ice bubbles until a maximum high is reached (**Figure 6.13**). Those bunches worsen the aerodynamic quality by raising the roughness. This leads to higher water collection efficiency and an altered convective heat transfer. The surface roughness is highest at the stagnation point and lowers towards the end of the curvature. (**Figure 6.15**)
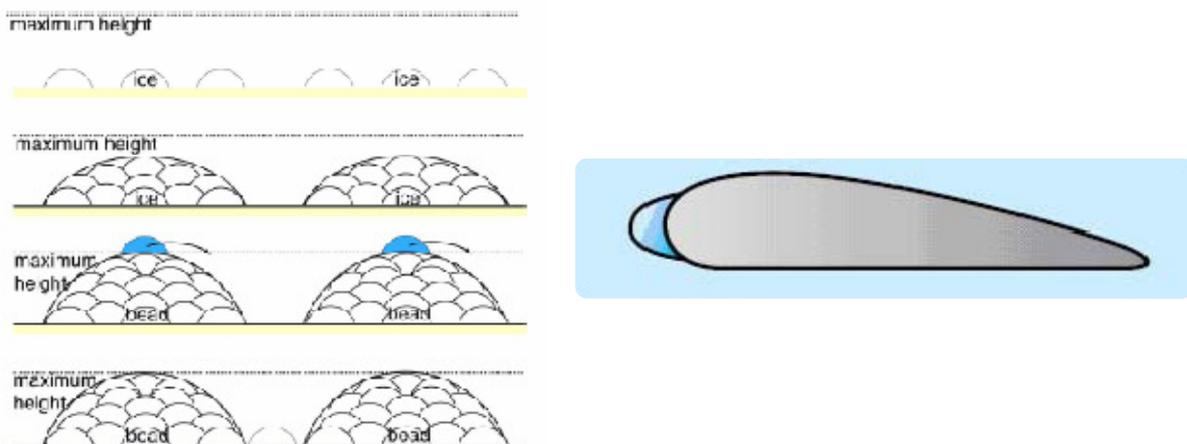
Figure 6.13   Rime ice accretions and shape
                            (Majed 2006)

6.5.2   Glaze ice

Higher temperature, the resulting runback water change the behavior and appearance of glaze ice shapes. On impact both ice and water leads to smooth zones around stagnation point and beads at the transition point **(Majed 2006).**   The beads grow by impinging droplets and receiving runback water from the zone before. The runback water flows around the airfoil constrained by aerodynamic forces and fills up gaps between still frozen parts. (**Figure 6.14**) The surface roughness is lowest at the stagnation point and enlarged towards the end of the curvature and ends of course at the end of the ice shape. So there will be expect substantial performance degradation (**Figure 6.15**)
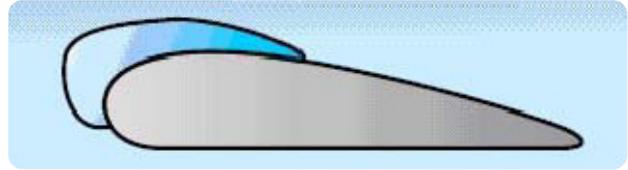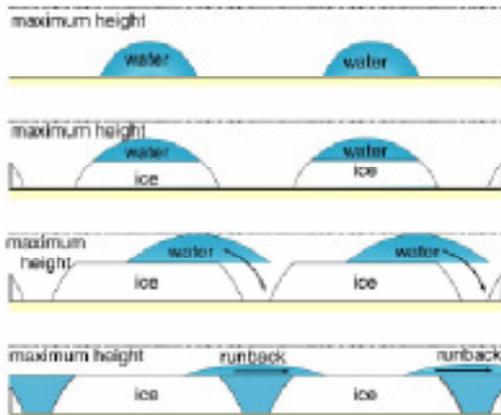
Figure 6.14   Glaze ice accretions and shape
(Majed 2006)

Rime ice conditions

- Air temperature: Low
- Airspeed: Low
- Liquid Water Content: Low
- Water droplets: Freeze on impact
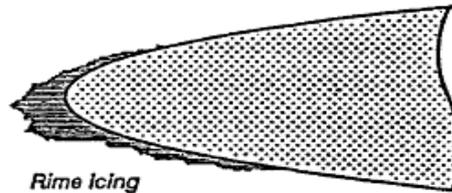
Rime icing

Glaze ice conditions

- Air temperature: High
- Airspeed: high
- Liquid Water Content: High
- Water droplets: Only a fraction freezes on impact, some flow on surface

Runback
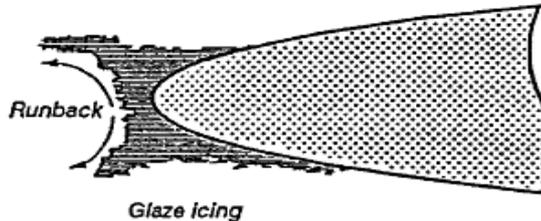
Glaze icing

Figure 6.15   Typical rime and glaze growth on an airfoil
(BRAGG 2002)

6.6   Summary of icing conditions and formation

Summarized the icing origin, process and types are a very complex subject which are here mentioned only basically. It can be seen that the ice prediction depends on many variables and computing icing accretions and indirectly the energy that is needed to de-ice the airfoil. It is possible that during the flight different icing or simultaneous condition can occur. For example as we see from the explanation of icing mechanism the ice possibility increases with increasing air stream velocity. Hence the physics of ice formation are particularly complex, it is difficult to predict precisely.

In the CS-25 the EASA describes rules and condition which aircraft has to been passing to be certified. Those rules are conservative and describe two conditions which aircraft engineers have to consider during the first design process. In summary there is a lot potential for investigation to get better results in ice prediction and improve certification process by being able to give exacter design point and interaction phenomena. Finally advancement comes t benefit pre-dimensioning to improve the early design process.

7   Conclusion

The DLRK paper deals with the pre-dimensioning of electrical de-icing system in order to predict fist power assumptions. It has been shown that with some constraints and assumptions a short and convenient equation can be accomplished. With Equation (4) it becomes possible to estimate the power requirement of an electro-thermal cyclic deicing system without defining a heater layout and a deicing sequence in advance. By estimating the k-factors in combination with empirical values of specific power requirements (either from literature or from this paper), the overall calculation becomes very short and convenient. Thus, a first statement of the system's required power load (either specific or overall) can be accomplished very easily. Parameters stated in Equation (18) are strictly true only for the stated Boeing 787. The results of the 787 power assumptions shows one more time that electrical overall de-icing requires a lot of energy. However, the k-factors might be considered as first estimate for trade studies and other further calculations. Of course with the assumptions further validations and meditations has to been made. The swept wing of commercial aircrafts could be having more influence than considered (here only in TAS). So the parameters can be adapted and corrected to gain better results (heating efficiency 70%, melted ice mass: 0.5mm).

In conclusion the CFD physics behind ice accretions are very complex and some of them are not very well known. So assumptions have to be made in order to solve this complex problem numerically. Current models work well for a wide range of cases but sometimes they have problems to predict the experimental results. Today's ice accretion codes are good in the prediction of ice catch rates, local and global collection efficiencies to determine the amount of energy for de-icing. Improvements are still being wanted in order to predict ice shapes that are as close to natural shapes. Basically the progress in developing computational tools for icing effects has been real slow so for the future better progress is needed in this important sector.

The physics behind the icing process are shown in chapter 6 and are basically explained. It is obvious that defining an icing design point for save aircraft operation is very serious due to the difficult icing prediction. Natural cloud formations contain different icing types and conditions which can be only approximately forecasted. Despite of the outer conditions the flight level, aircraft configuration and e.g. flight speed could affect the accretion formation. The EASA defines various icing conditions for commercial aircraft manufacturer to face these hazardous conditions and take them into account during the design process. Those conditions can be consulted to design de-icing systems, create tests for natural icing test whether in icing tunnels or flight test and create numerical methods to improve the icing and power prediction. In the future with cooperation of CFD we will be able to understand icing physics and the prediction of icing conditions better to make sure that aircrafts can be operated safely in hard weather conditions.

8   Acknowledgement

References

Al-Khalil 1997   AL-KHALIL, K.; HORVATH, C.: AIAA1997-0051: *Validation of Thermal Ice Protection Computer Codes: Part 3-The Validation of ANTICE*, 35th Aerospace Sciences Meeting & Exhibit, Reno,NV, January 6-7, 1997

Al-Khalil 2007   AL-KHALIL, Kamel: *Thermo-Mechanical Expulsion Deicing Systems – TMEDS.* In: 45th AIAA Aerospace Sciences Meeting and Exhibit   , Reno, Nevada, 8 - 11 January, 2007
-       URL:http://www.coxandco.com/engineering/pdf/AIAA-2007-0692.pdf (2010-06-10)

Bigarré 2003   BIGARRÉ, Capt. Jean-Michel: *Be Prepared for Icing*, ATR brochure 2003
-       URL: http://www.scribd.com/doc/6822925/Icing2003 (2010-08-25)

Bragg 2002   BRAGG, M. B.; PARASCHIVOIU, I.; SAEED. F.: *Aircraft Icing*, A Wiley-Interscience, Publication, New York, 2002

CW 2008   ARTICLE: *787 integrates new composite wing deicing system, 12/30/2008*
-       URL: http://www.compositesworld.com/articles/787-integrates-new- composite-wing-deicing-system (2010-09-01)

EASA 2008   EUROPEAN AVIATION SAFETY AGENCY: *Certification Specifications for Large Aeroplanes CS-25*, Amendment 5, CS-25 Book 1. EASA, 2008

Gehrer 1999   GEHRER, A.: *Entwicklung eines 3D-Navier-Stokes Codes zur numerischen Berechnung der Turbomaschinenströmung,* Dissertation an der Fakultät für Maschinenbau der TU Graz, 1999
-       URL: http://ttm.tugraz.at/arno/arno-paper.html   (2010-08-05)

Habashi 2002   HABASHI, Wagdi G.; TRAN, Pascal; BARUZZI, Guido; AUBÉ, Martin; BENQUET, Pascal: *Design of Ice Protection Systems and Icing Certification Through the FENSAP-ICE System*, Newmerical Technologies, Paper, Paris, France, published in RTO-MP-089, 22-25 April 2002

Habashi 2004   HABASHI, Wagdi G.: *CFD*: *Pacing In-flight Icing Simulation, A Workshop in Honor of Antony Jameson's 70-year-young B-day,* NSERC-J. Armand Bombardier Industrial Research Chair of Multidisciplinary CFD McGill University, 2004

Incropera 2007   INCROPERA, Frank P.: *Fundamentals of heat and mass transfer.* Hoboken, NJ : Wiley, 2007

Klimedia 2010   UNIVERSITÄT BERN, Klimedia: *Der Sättigungsdampfdruck*, 05/10/2010
-          URL: http://www.klimedia.ch/kap3/a11.html (2010/08/10)

La Burthe 2010   LA BURTHE, Claudius: *Understanding the process of ice accretion*,
-          URL: http://pilotlab.net/library-2/meteorology/ (2010-09-15)

LTH 2008   LTH: *Die Vereisung von Flugzeugen*, Luftfahrttechnisches Handbuch (AD 07 03 001), Ausgabe A, LTH Koordinierungsstelle, Ottobrunn: IABG, 2008

Majed 2006   SAMMAK, Majed: *Anti-icing in gas turbines*, Thesis for the Degree of Master of Science, Department of Heat and Power Engineering, Lund Institute of Technology, Lund University, Sweden, February 2006
-          URL: http://www.vok.lth.se (2010-05-04)

Paraschivoiu 2001   PARASCHIVOIU, Ion; SAEED, Farooq: *Ice Accretion Simulation Code CANICE*, École Polytechnique de Montréal, Montréal, Canada, 2001

SAE 1990   SAE: *Ice, Rain, Fog, and Frost Protection*. Warrendale, PA : Society of Automotive Engineers, 1990 **(AIR 1168/4)**. – Available from Technische Universitätsbibliothek Hamburg-Harburg (signature: 3210-1320)

Scholz 2007   SCHOLZ, Dieter: *Aircraft Systems Lecture Notes*, Hamburg University of Applied Sciences, Dept. of Automotive and Aeronautical Engineering. Lecture Notes,2007

Sherif 1997   SHERIF, S.A.; PASUMARTHI, N.; BARTLETT, C.S.: *A semi-empirical model for heat transfer and ice accretion on aircraft wings in supercooled clouds*, Cold Regions Science and Technology 26 (1997) S.165-17

Sinnett 2010   SINNETT, Mike: *787 No-Bleed Systems:*
Saving Fuel and Enhancing Operational Efficiencies, Aeromagazine
04 | 07,
-        URL: www.boeing.com/commercial/ (2010-07-23)

Wright 1997   WRIGHT, William B.; AL-KHALIL, Kamel; MILLER, Dean:
Validation of NASA Thermal Ice Protection Computer Codes Part 2 -
LEWICE/Thermal, Brook Park, OH, 1997

Appendix A –

DLRK2010 Paper

A HANDBOOK METHOD FOR THE ESTIMATION OF POWER REQUIREMENTS FOR ELECTRICAL DE-ICING SYSTEMS

O. Meier, D. Scholz
Hamburg University of Applied Sciences
Aero – Aircraft Design and Systems Group
Berliner Tor 9, 20099 Hamburg

Abstract

Electrical de-icing consumes more power than is generally available from the generators. Therefore, electrical de-icing only becomes feasible, if the power is merely used during limited time intervals to melt the ice and separate it from the wing. The airflow then simply carries the ice away which avoids the need for further power to melt or even evaporate the ice totally. The ice slabs forming on the wing can be carried away by the airflow, if the slabs are separated from one another. Separation is achieved by constantly heated parting strips. This paper provides an easy to use method to estimate power requirements for such electrical de-icing systems taking account of described power saving technologies. In contrast to an established method by SAE, equations are derived here from first principles and SI units are applied. Based on the example of the Boeing 787 aggregated general technology parameters (k-factors) are derived. Applying these Boeing 787-based k-factors power estimations for other similar aircraft are greatly simplified. Without own experimental results for verification, the method is eventually calibrated based on findings published in the literature and own assumptions. Example calculations yield power requirements in the right order of magnitude. Based on the calculations of this paper the Boeing 787 would require 3.61 kW/m² for de-icing. The total required installed power for a Boeing 787 with an electrical de-icing system (and technologies as described) would be 75.8 kW which is in good agreement with the published power range of 45 to 75 kW.

NOMENCLATURES

e_{surf} iced wing span $[\mathrm{m}]$

c_{ice} heat capacity of ice $\left[\dfrac{\mathrm{kJ}}{\mathrm{kg\,K}}\right]$

c_{liqu} heat capacity of water $\left[\dfrac{\mathrm{kJ}}{\mathrm{kg\,K}}\right]$

cp_{air} specific heat capacity $\left[\dfrac{\mathrm{kJ}}{\mathrm{kg\,K}}\right]$

E_m water catch efficiency $[1]$

e_{∞} ambient saturation pressure $[\mathrm{Pa}]$

e_{surf} surface saturation pressure $[\mathrm{Pa}]$

h_0 local heat transfer coefficient $\left[\dfrac{\mathrm{W}}{\mathrm{m^3\,K}}\right]$

k_0 thermal conductivity of air $\left[\dfrac{\mathrm{W}}{\mathrm{m\,K}}\right]$

k_{cycl} total cycle time factor $[1]$

k_{ps} parting strip factor $[1]$

L_e latent heat of vaporization $\left[\dfrac{\mathrm{kJ}}{\mathrm{kg}}\right]$

L_f latent heat of fusion $\left[\dfrac{\mathrm{kJ}}{\mathrm{kg}}\right]$

$\dot{m}_{local}$ local water catch $\left[\dfrac{\mathrm{kg}}{\mathrm{s\,m^2}}\right]$

Nu Nusselt number $[1]$

n freezing fraction $[1]$

p_{∞} ambient air pressure $[\mathrm{Pa}]$

Pr Prandtl number $[1]$

P_{req} required electrical power $[\mathrm{W}]$

P_{elec} available. electrical power $[\mathrm{W}]$

q_{AII} overall heat $\left[\dfrac{\mathrm{kW}}{\mathrm{m^2}}\right]$

q_{KE} kinetic heating $\left[\dfrac{\mathrm{kW}}{\mathrm{m^2}}\right]$

q_{aero} aerodynamic heating $\left[\dfrac{\mathrm{kW}}{\mathrm{m^2}}\right]$

q_{convec} convective heating $\left[\dfrac{\mathrm{kW}}{\mathrm{m^2}}\right]$

q_{evap} evaporative heating $\left[\dfrac{\mathrm{kW}}{\mathrm{m^2}}\right]$

$q_{sensible}$ sensible heating $\left[\dfrac{\mathrm{kW}}{\mathrm{m^2}}\right]$

R_h relative humidity $[1]$

R_c boundary recovery factor $[1]$

$R_{e,p}$ Reynolds Number $[1]$

T_{∞} ambient Temperature $[\mathrm{K}]$

T_{MSL} air temperature at mean sea level $[\mathrm{K}]$

T_{sk} skin Temperature $[\mathrm{K}]$

t maximum airfoil thickness $[\mathrm{m}]$

v_{TAS} true air speed $\left[\dfrac{\mathrm{m}}{\mathrm{s}}\right]$

ρ_{LWC} mass of supercooled water p. vol. $\left[\dfrac{\mathrm{kg}}{\mathrm{m}^3}\right]$

ABBREVIATIONS

AIR   Aerospace Information Reports
CS   Certification Specifications
FAA   Federal Aviation Administration
SAE   Society of Automotive Engineers

1. INTRODUCTION

"Power by Wire", the "All Electric Aircraft" or the "More Electric Aircraft" have been discussed for years. The application of these concepts in civil aviation however was much delayed by the fact that in an "All Electric Aircraft" not only power generation but also all consumers have to be electrical. For example the introduction of electrical primary flight controls, braking systems or de-icing systems has seen many challenges and their overall economical benefits were often unclear.

In order to prove the benefits of electrical systems, trade-off studies are always necessary. These trade-off studies are required already in the very early phases of an aircraft project. These early phases of a project are characterized by a lack of data and very limited investigation time. Often many system variants have to be checked with a limited amount of engineering man power. Quick and easy to use handbook methods are generally a good way to work within such a situation.

2. AIM, APPROACH AND APPLICATION

The aim of this paper is to estimate **power requirements** for electrical de-icing systems. Literature was checked for available existing handbook methods. An understanding from first **thermodynamic principles** was sought and the use of SI units self-evident. The handbook method from this paper should be so simple that it can be part of the preparation of trade-off studies. **Trade-off studies** compare various design principle with one another during early aircraft development. Hence many quick calculations for one aircraft project with very little time need to be supported.

3. CLASSIFICATION OF THERMAL ICE PROTECTION SYSTEMS

Ice protection is achieved mostly with **thermal** systems. Other means of ice protection are possible. The ice protection on large turbo prop aircraft is done with **mechanical** systems: Ice is shed by rubber boots that inflate due to applied internal air pressure. This paper only considers thermal ice protection.

It is differentiated between de-icing and anti-icing. The terms are defined in AIR 1168/4 [1]:

* **De-icing** is the periodic shedding, either by mechanical or thermal means, of small ice buildups by destroying the bond between the ice and the protected surface.

* **Anti-icing** is the prevention of ice buildup on the protected surface, either by evaporating the impinging water or by allowing it to run back and freeze on noncritical areas.

Thermal ice protection systems are classified according to three principals:

1. **Evaporative anti-icing systems** supply sufficient heat to evaporate all water droplets impinging upon the heated surface.

2. **Running-wet anti-icing systems** provide only enough heat to prevent freezing on the heated surface. Beyond the heated surface of a running-wet system, the water can freeze, resulting in runback ice. Running-wet systems must be designed carefully so as not to permit buildup for runback ice in critical locations.

3. **Cyclic de-icing systems** periodically shed small ice buildups by melting the surface-ice interface with a high rate of heat input. When the adhesion at the interface becomes zero, aerodynamic or centrifugal forces remove the ice.

An evaporative anticing system uses the most energy of the three ice protection principles presented, cyclic de-icing uses the least energy.

4. CONVENTIONAL THERMAL ICE PROTECTION OF TODAY'S JET AIRCRAFT

Jet aircraft are classically provided with thermal ice protection systems. Ice protection of larger surfaces of these aircraft is done with pneumatic power. **Pneumatic power** is taken as bleed air from the aircraft engines and holds sufficient power for de-icing (Figure 1). The engine bleed air system extracts pressurized air from one or more bleed ports at different stages of the engine compressor of each engine on the aircraft. The bleed air system controls the pressure and temperature of the air and delivers it to a distribution manifold. The pressure is

controlled by a pressure-regulating valve, and the temperature is lowered in a precooler with fan air or ram air.

The engine bleed air system supplies the hot air to the anti-ice system. The Airbus A321 wing **ice protection** system (Figure 4) is a thermal (hot air) evaporative anti-ice system. Only slats 3, 4, and 5 on the outboard wing need to be ice protected on this aircraft. An anti-ice valve isolates the anti-ice system from the bleed air supply. Ducts connect the anti-ice valve to a telescopic duct at slat 3. A piccolo tube runs along slat 3, 4, and 5 and supplies the hot air to the leading edge. A piccolo tube is a tube with calibrated holes that ensures that hot air is evenly distributed along the leading edge, although bleed pressure decreases towards the wing tip. The bleed air in the slats is released overboard through the holes in the bottom surface of the slat.
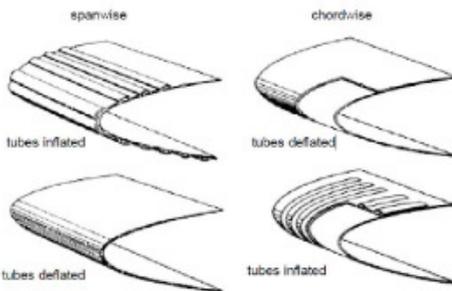
FIG 1: FAA: boot surfaces

5. PRESENT AND FUTURE CYCLIC ELECTRICAL WING DE-ICING SYSTEMS

Electrical power is taken from generators on board the aircraft. Generators are often engine driven, but can provide considerably less power than the available pneumatic power, taken as bleed air from the engine (compare with Section 4) [2]. Electrical de-icing of larger components or surfaces can hence cause a problem due to (maybe too) high power demands [3].

Cyclic electrical de-icing is only possible with a combination of (see Figure 2) [4]:

a) surfaces that are only heated during some time intervals (**cyclic heated surfaces**) just melting the bonding contact area of the ice and with

b) permanently heated **parting strips** ensuring separation of the ice layers, which are finally carried away by the air stream.

Cyclic electrical de-icing [4] saves energy because only a small portion of the ice is actually melted. Most of the ice leaves the aircraft in solid form.

The intention of this paper is to calculate the power requirements of cyclic electrical de-icing systems as presented in Figure 2 by means of a simple handbook method (see Section 10).
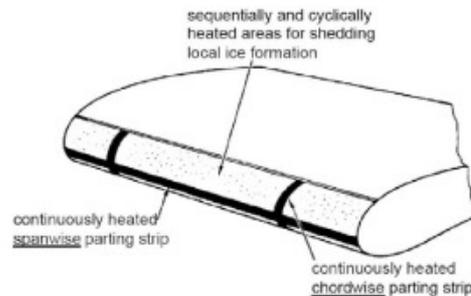
FIG 2: Arrangement of a wing area with electric cyclic de-icing (from [5], p. 9-9).

6. ICING FUNDAMENTALS

(Liquid) water below 0 °C is called supercooled water. Supercooled water can exist because the water has been totally undisturbed during cooling – nothing has caused it to turn to ice. When an aircraft hits the droplet, however, the droplet receives the necessary input for the phase change and turns to ice. The phase change from water to ice requires some latent heat extraction, but when the droplets are supercooled water, the heat extraction has already taken place. The ice water mixture will be slightly warmer than the supercooled water was just a second earlier. Hence: Supercooled water turns instantly to ice due to the interaction with the aircraft.

7. STATE-OF-THE-ART IN HANDBOOK METHODS

Only one handbook method seems to exist that is readily available. It is published by SAE [1]:

SAE: *Ice, Rain, Fog, and Frost Protection.* Warrendale, PA : Society of Automotive Engineers, 1990 (AIR 1168/4)

This method is mainly based on empirical equations. An approach based on internationally known equations from thermodynamics and heat transfer based on first principles together with the use of SI units would be beneficial.

8. ASSUMPTIONS FOR A HANDBOOK METHOD

Detailed simulations of ice accretion on airfoils are already used in industry. There are many different numerical approaches to calculate ice shapes for various atmospheric and flight conditions. Several two-dimensional and three-dimensional ice accretion codes have been developed. A literature review is given in [6] and [7].

In contrast to these numerical codes, a quick and easy to use handbook method inevitably has to make simplifying assumptions:

- Only two dimensional effects are considered.

- Only one point along the airfoil's leading edge is evaluated. Reynolds number, static pressure, temperature, water catch etc. are different in magnitude and direction at each point of the wing. Average values are used.

- The overall cyclic power requirement is the integrated value over all local cyclic power requirements taking into account the time fraction of cyclic surface heating and the relative surface area of the parting strips.

- Power requirements for de-icing depend on atmospheric conditions [8]. Certification rules from CS-25 [9] require the calculation of various design points with different e.g. ambient temperatures, liquid water contents, droplet diameters on the one hand and flight speeds v and airfoil thickness t on the other hand (Figure 3). The handbook method only considers one design point that is considered critical.
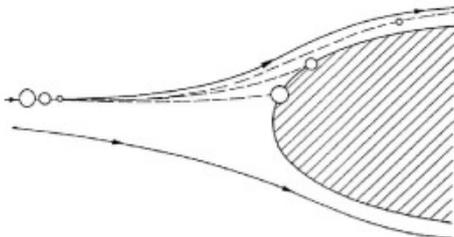
FIG 3: Not all droplets impinge on the wing surface. This fact is expressed by the water catch efficiency, [5]

9. SIMPLIFIED WATER CATCH CALCULATION

In order to calculate the total water catch of the wing, let us cut off a piece of a wing with a spanwise extension Δy and maximum thickness t. This piece of wing may fly at a speed v through a volume of air with a certain mass of supercooled water. The mass of supercooled water per volume is called *liquid water content* (LWC) and is something like a density named ρ_{LWC}. We consider $t \Delta y$ as the area of an imaginary sieve at an angle perpendicular to its flight path. The mass flow rate of supercooled water through the sieve would be as much as $\dot{m} = v t \Delta y \rho_{LWC}$. The impingement of water on the leading edge of the wing will, however, be different from the flow through the sieve as shown in Figure 3 The air and with it very small droplets pass around the wing; only larger droplets hit the surface. This phenomenon is expressed by the water catch efficiency E_m. The imaginary sieve shows an efficiency $E_m = 1$. The water catch at a certain spanwise location y and a spanwise extension Δy on the wing is calculated by

(1) $\dot{m} = v t \rho_{LWC} E_m$

E_m is a function of aircraft speed and droplet size, airfoil thickness and shape, viscosity and density of the air:

- High aircraft velocities and a large droplet size cause an increase in water catch efficiency.

- Thin wings divert the flow less and increase the water catch efficiency.

AIR 1168/4 [1] presents detailed methods to calculate E_m.

A simplified method to calculate the water catch efficiency E_m is presented here based on Figure 3F-3 of AIR 1168/4 [1] as a function of aircraft speed v and wing thickness t (Figure 5). Based on typical airfoils with a relative thickness of 6 ... 16 % at an angle of attack of $\alpha = 4$ °, a simplified formula for calculating E_m is presented:

(2) $E_m = 0.00324 \left(\dfrac{v}{t} \right)^{0.613}$

for v in m/s and t in m .

This formular is strictly true for $d_{med} = 20\ \mu m$ and an altitude of $h = 10000\ ft$. Other altitudes from sea level to $h = 20000\ ft$ will result in error lass than 10 %. For a simple method, we do not distinguish between difference due to spanwise location. For the total wing it is $\Delta y = b$ where b is the wing span. The total water catch of the wing is thus calculated by

(3) $\dot{m} = v t b \rho_{LWC} E_m$

10. CALCULATION OF POWER REQUIREMENTS

10.1 Calculation of Power Requirements for Continuously Heated Surfaces

The **parting strips** (presented in Section 5) are continuously heated surfaces. They are heated to a defined constant temperature. It is assumed here that this temperature is 6 °C. This temperature is sufficient to prevent the surface from freezing.

The surface is bombarded with supercooled droplets that turn partially into ice. It is interesting to note that at e.g. -18 °C only 22 % of the water will be ice after impact. No matter if ice or water, the supercooled H_2O needs to be warmed up and that requires a heat flow.

The heat flow per unit area $\dot{q}$ required to keep the parting strips free of ice can be expressed by an energy balance [10], [11] for each surface element on the wing. In the simplest form, the energy required by an anti-icing system is determined from the rate that must be supplied to balance the heat losses from the heated surface. In detail there is sensible heating, convective cooling, and evaporative cooling. In contrast, the kinetic heating due to droplets that are coming to rest when striking the surface do have a positive influence, thus heating up the surface and lowering the required heat flow. The same is true for aerodynamic heating. The required heat flow for anti-icing (A/I) is similar to the parting strips heat flow [12], [11] thus calculated from

$$(4) \quad \dot{q}_{A/I} = \dot{q}_{PS} = \dot{q}_{sens} + \dot{q}_{conv} + \dot{q}_{evap} + \dot{q}_{kin} + \dot{q}_{aero}$$

a) Sensible Heating

The supercooled droplets impinging at a mass flow per unit area of the imaginary sieve $\dot{m}_{local}$ have to be heated up to the surface temperature. The ice must additionally first become liquid; latent heat needs to be added. With freezing fraction n which indicates the amount of liquid water that turns into ice:

$$(5) \quad \dot{q}_{sensible} = \dot{m}_{local}[\Delta T((1-n)c_{liq} + nc_{ice}) + nL_f]$$

$$(6) \quad E_m = 0.00324\left(\frac{v}{t}\right)^{0.613}$$

$$(7) \quad \dot{m}_{local} = v \rho_{LWC} E_m$$

a) Convection

The convective heat loss can be calculated from

$$(8) \quad \dot{q}_{convec} = h_0(T_{skin} - T_\infty)$$

Where h_0 is the local heat transfer coefficient.

$$(9) \quad h_0 = Nu\frac{k_0}{x}$$

with $\quad k_0 = 0.0227\frac{W}{mK} \quad$ for air at 255.3 K.

The dimensionless quantities are calculated as follows:

Nusselt number:

$$(10) \quad Nu = 0.0296 \cdot Re_x^{\frac{4}{5}} \cdot Pr^{\frac{1}{3}}$$

Prandtl number:

$$(11) \quad Pr = \frac{c_p \mu}{k_0}$$

Reynolds number:

$$(12) \quad Re = \frac{\rho_{MSL} v l}{\mu}$$

c) Evaporation

The evaporative heat loss equals the rate of mass evaporated from the surface multiplied by the latent heat of evaporation. For fully evaporative anti-icing the surface is heated sufficiently to evaporate all of the impinging supercooled liquid water. For a running-wet system, however, the surface water is only partially evaporated. How much of the water evaporates depends not only on the surface temperature but also on the saturation pressure e [13] as well as on relative humidity R_h. The latent heat for water evaporation is $\quad L_e = 2257\frac{kJ}{kg}$.

In literature many equations can be found to calculate the saturation pressure

$$(10) \quad \dot{q}_{evap} = 0.7 h_0 L_e \frac{R_h e_\infty - e_{surf}}{p_\infty c_{p,air}}$$

$$(11) \quad e = \frac{f}{100} 6.107 \, 10^{7.5\frac{T}{237+T}}$$

TAB 1. Results of specific parting strip power requirements

source	$\dot{q}_{PS}$ [kW/m²]	t [C°]
Example Calculation for parting strip power requirements	11.82	-17.78
AIR 1168/4 calculation scheme	14.13	-17.78
AIR 1168/4 suggested value (p. 28)	18.6	-17.78

d) **Kinetic Heating**
Heat gain due to the impinging accelerated super cooled droplets.

$$(12) \quad \dot{q}_{KE} = \dot{m}_{local} \frac{v_\infty^2}{2}$$

e) **Aerodynamic Heating**
Heat gain due to friction in the boundary layer over the surface. Like with all other heat gains, power requirements for the de-icing system are lowered due to heat gains. Hence, at high aircraft speeds no more ice protection is needed.

$$(13) \quad \dot{q}_{aero} = R_c h_0 \frac{v_\infty^2}{2 c_{p,air}}$$

R_c represent the boundary recovery factor with $n = 0.5$ due to laminar boundary layer [12].

$$(14) \quad R_c = 1 - \left(\frac{0.99 \; v_1^2}{v_\infty^2} \right) (1 - Pr^n)$$

In all of the calculations (a) to (e) various aircraft depending and environment depending parameters are required as input. A calculation is only possible with a certain aircraft and and icing condition in mind. As an example, parameters listed below have most likely a keen influence on running wet anti-icing (and thus on the parting strip) power requirements:

- atmospheric icing conditions (continuous maximum or intermittent maximum)
- true air speed
- ambient temperature
- pressure altitude
- mean effective drop diameter (20 μm)
- airfoil geometry
- Reynolds number

- heater layout / geometry

Using Boeing 787 parameters and dimensioning icing conditions from CS-25, specific power requirements can be calculated and are given an compared with values from literature in Table 1.

10.2 Calculation of power requirements for cyclic heated surfaces.

- To calculate cyclic power requirements, the unheated equilibrium temperature has to be assumed (6 °C).

- The amount of ice to be melted to destroy the bond between the ice and the airfoil varies with the considered position along the airfoil (stagnation point, etc.). An average value of 0,5 mm has been assumed due to general considerations and coincides the over all de-icing performance of Boeings 787 [3].

- Some of the supplied heat is not reaching the ice but is lost to the environment via the aircraft structure. The efficiency is assumed to be 70 %.

With the following equation it becomes more convenient:

$$(15) \quad \dot{q}_{sensible} = \dot{q}_{Cycl} = \frac{\dot{m}_{ice}}{t} [\Delta T c_{Ice} + L_f]$$

With:

$$(16) \quad m_{ice} = t \rho$$

Thus, per square meter, a mass of 0.45 kg of ice has to be melted. With the assumptions from above this yields a specific power requirement as given and compared in Table 2. The calculated value is not dependent on any aircraft parameters.

Compared to the AIR 1168/4 value the computed one it is very low due to the adopted water film who is responsible for the ice slip of.

TAB 2. Results of specific parting strip power requirements

source	$\dot{q}_{Cycl}$ [kW/m²]	t [C°]
Calculated	27.25	-17.78
AIR 1168/4 (p. 28)	34.10	-17.78

10.3 Calculation of Power Requirements for a Generic Heater Layout

It can be noticed that the method of cyclic deicing with parting strips an shown in Fig. 2 uses two basic principles:

- decrease of the continuously heated area (parting strips), and

- decrease of the heat-on time (cyclic deicing).

In order to calculate the overall (average) specific heat flow, it is NOT necessary to know the detailed layout of the de-icing system. Only two factors are required:

- k_{PS} gives the ratio of the area of continuously heated parting strips against total area to be de-iced. A given layout shows 19 % area covered with parting strips.

- k_{cycl} gives the ratio of cyclic heat on time against total cycle time. From AIR 1168/4 we take 9 s heat-on-time in a 3 min. = 180 s cycle time. This is 5 % heat-on-time.

$$(17) \quad \dot{q}_{total} = \dot{q}_{PS} \cdot k_{PS} + \dot{q}_{cycl} \cdot k_{cycl}$$

For the k-factors as given above the average heat load is **3.61 kW/m²**. Other heater layouts and heating cycles will have other heat loads. The value of **3.61 kW/m²** is the result from this paper based on assumptions, general thermodynamic equations and considered parameters ([9], [1]).

11. ABSOLUTE POWER REQUIREMENTS FOR DE-ICING

Based upon the generic heating performance the absolute power requirements can be estimated. With parameters of the Boeing 787 and its heated leading edge area a calculation is possible for the area of the imaginary sieve.

$$(18) \quad S_{ice} = t \ b_{ice}$$

With parameters for the B787: $S_{ice} = 20.95 \text{m}^2$

Based on the definition in 10.1 a) the required power is calculated from

$$(19) \quad P_{req} = \dot{q}_{total} \ S_{ice}$$

The computation of required power respects that 8 slats could be energized cyclically (sequentially). Based on AIR 1168/4 k_{cycl} is taken as 5 %. With the dimensions of Boeing's new 787 with 8 heated slats:

$$(20) \quad P_{req,cycl} = 75.8 \text{kW}$$

Surfaces on the B787 can also be heated simultaneously. In this case $k_{cycl} = 1$ and

$$(21) \quad P_{req,simul} = 247.4 \text{kW}$$

These values may be compared with the available electrical power on board the B787. All B787 generators produce together

$$(22) \quad P_{elec} = 1000 \text{kVA}$$

12. SUMMARY AND RECOMMENDATIONS

This paper deals with the pre-dimensioning of electrical de-icing system in order to predict the power consumption of the system. Based on some constraints and assumptions a final and simple equation (17) was derived. With this equation it becomes possible to estimate the power requirement of an electro-thermal cyclic deicing system without defining a heater layout and a deicing sequence in advance. By estimating the k-factors in combination with empirical values of specific power requirements (either from literature or from this paper) the overall calculation becomes very efficient. Thus, a first statement of the system's required power load (either specific or overall) can be accomplished very fast and easy. Parameters for the sum of all heat flows - Equation (4) - are strictly true for the conditions as selected in this paper. Compared with results from **AIR 1168/4** the computed results as given in TAB 1 and TAB 2 differ only about 16 % for continuously heated surfaces $(\dot{q}_{All} = \dot{q}_{PS})$ and 20 % for cyclic heated surfaces $(\dot{q}_{Cycl})$. The calculated power requirements for the B787 indicate one more time that electrical wing de-icing requires a lot of energy or an intelligent layout of the system. At the chosen design point and with selected assumptions the computed results (75.8 kW) are in good agreement with published data [3] (45-75 kW). It also turned out that design parameters like slat chord c_{slat} or airfoil thickness t affect the results only marginally so that for preliminary computing a preliminary geometry can be used.

The k-factors may be considered as first estimates for trade studies and other preliminary calculations. Of course once the detailed layout for a specific electric wing heating system is known the k-factors have to be recalculated. Also the parameters $\dot{q}_{PS}$ and $\dot{q}_{cycl}$ can be adapted and corrected to gain better results. Here crucial input parameters are the heating efficiency (taken as 70 %) and the melted

72

ice layer thickness (taken as 0.5 mm). These values were identified from the known power consumption of the B787 together with data from AIR 1168/4 and logical coherence's. The 3D effect of the wing has not been considered. In this paper it was just assumed that the flow passes through an area projected into the flow direction. Further investigations could look closer into the effects of a swept wing on icing.

LIST OF REFERENCES

[1] SAE: *Ice, Rain, Fog, and Frost Protection.* Warrendale, PA : Society of Automotive Engineers, 1990 (AIR 1168/4)

[2] SINNETT, M.; Director, 787 Systems, *787 No-Bleed Systems: Saving Fuel and Enhancing Operational Efficiencies*, aeromagazine quarterly q tr_04|07, URL: www.boeing.com/commercial/

[3] COMPOSITESWORLD; *787: integrates new composite wing deicing-system*, URL:http://www.compositesworld.com/articles/787-integrates-new-composite-wing-deicing-system, 12/30/2008

[4] AL-KHALIL,Kamel:*Thermo-Mechanical Expulsion Deicing Systems – TMEDS*. In: 45th AIAA Aerospace Sciences Meeting and Exhibit 8 – 11 January,Reno,Nevad, URL:http://www.coxandco.com/engineering/pdf/AIAA-2007-0692.pdf

[5] SCHOLZ, D.: *Aircraft Systems Lecture Notes*, Hamburg Universityof Applied Sciences, Dept. of Automotive and Aeronautical Engineering. Lecture Notes, 2007

[6] AL-KHALIL, K.; HORVATH,C.; AIAA1997-0051: *Validation of Thermal Ice Protection Computer Codes: Part 3 - The Validation of ANTICE*, 35th AerospaceSciences Meeting & Exhibit, Reno, NV, 1997

[7] HABASHI,W. G.; TRAN,P.; Baruzzi,G.; AUBÉ M.; and BENQUET, P.: *Design of Ice Protection Systems and Icing Certification Through the FENSAP-ICE System*, Newmerical Technologies, Paper presented at the RTO AVT Symposium on "Reduction of Military Vehicle Acquisition Time and Cost through Advanced Modelling and Virtual Simulation",Paris, France, 22-25 April 2002

[8] SAMMAK M.; *Anti-icing in gas turbines, Thesis for the Degree of Master of Science February 2006, Department of Heat and Power Engineering*, Lund Institute of Technology, Lund University, Sweden, www.vok.lth.se

[9] EASA: *Certification Specifications for Large Aeroplanes CS-25*, Amendment 5, CS-25 Book 1. EASA, 2008

[10] INCROPERA, F.P.: *Fundamentals of heat and mass transfer*. 6. ed. Hoboken, NJ : Wiley, 2007

[11] LTH: *Die Vereisung von Flugzeugen. Luftfahrttechnisches Handbuch (AD 07 03 001), Ausgabe A*, LTH Koordinierungsstelle, Ottobrunn: IABG, 2008

[12] SHERIF,S.A.; PASUMARTHI, N.; BARTLETT ,C.S.; *A semi empirical model for heat transfer and ice accretion on aircraft wings in supercooled clouds*, Cold Regions Science and Technology (1997)

[13] KLIMEDIA, *Der Sättigungsdampfdruck*, URL:http://www.klimedia.ch/kap3/a11.html 05/10/2010
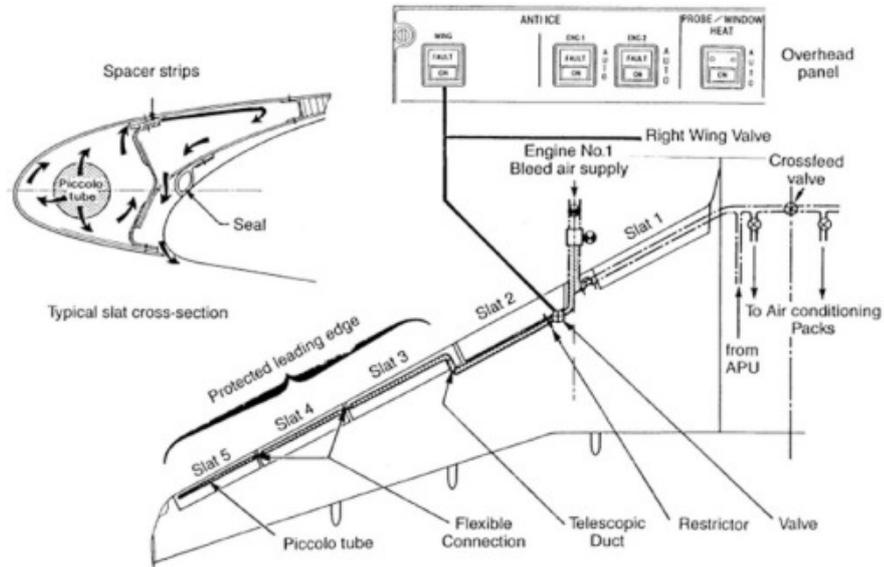
FIG 4: Wing anti-ice of an Airbus A321 (from [5], p. 9-15)
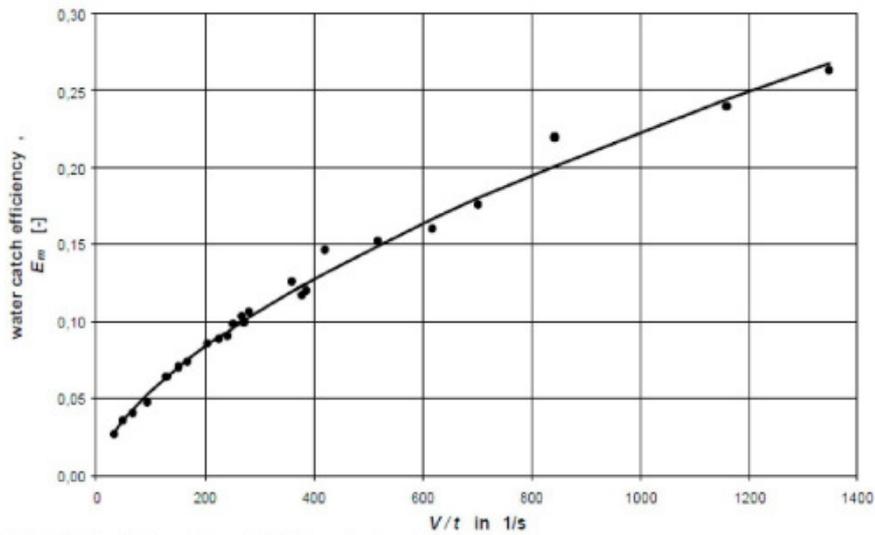
FIG 5: Catch efficiency rises with higher velocity and thinner airfoils.

Appendix B –

DLRK2010 Presentation

Hochschule für Angewandte Wissenschaften Hamburg
Hamburg University of Applied Sciences

AERO – AIRCRAFT DESIGN AND SYSTEMS GROUP

A HANDBOOK METHOD FOR THE ESTIMATION OF POWER REQUIREMENTS FOR ELECTRICAL DE-ICING SYSTEMS

Oliver Meier   Hamburg University of Applied Sciences
Dieter Scholz   Hamburg University of Applied Sciences

MOZART

MOZART –
Health Monitoring von
Brennstoffzellensystemen
in der Luftfahrt

Deutscher Luft- und Raumfahrtkongress 2010
German Aerospace Congress 2010
Hamburg, Germany, 31.8.-02.09.2010   DLRK2010-1291

Hochschule für Angewandte
Wissenschaften Hamburg
Hamburg University of Applied Sciences

A HANDBOOK METHOD FOR THE ESTIMATION OF POWER REQUIREMENTS FOR ELECTRICAL DE-ICING SYSTEMS

Contents

- Motivation
- Aim
- Today's Aircraft Anti-Icing and De-Icing Systems
- Present and Future Electrical Wing De-Icing Systems
- State-of-the-Art in Handbook Methods
- Assumptions for a Handbook Method
- Calculation of Power Requirements
  - Cyclically Heated Surfaces
  - Continuously Heated Surfaces
  - Generic Heater Layout
- Absolute Power Requirements for De-Icing
- Conclusion

Oliver Meier, Dieter Scholz
Electrical de-icing systems

Deutscher Luft- und Raumfahrtkongress
31.8.2010-02.09.2010 Hamburg

24.08.2010, Folie 2
Aero - Aircraft Design and Systems Group

A HANDBOOK METHOD FOR THE ESTIMATION OF POWER REQUIREMENTS FOR ELECTRICAL DE-ICING SYSTEMS

Motivation

- Vision of an "More Electric Aircraft"

- Mike Sinnett, Director, 787 Systems:
  "787 No-Bleed Systems: **Saving Fuel** and
  Enhancing Operational **Efficiencies**"

- Prove benefits in **trade off studies** during early
  phase of a project

- Required: Quick and easy to use **handbook
  method**
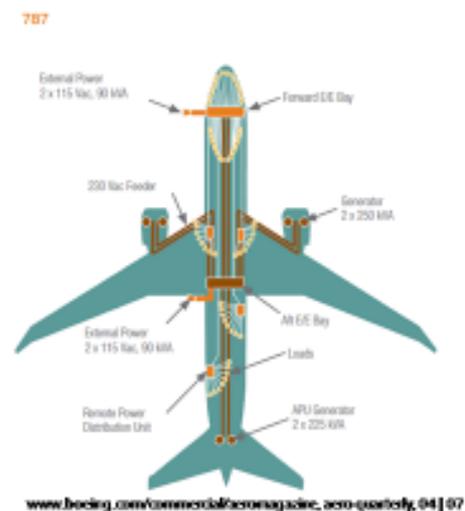
787

External Power
2 x 115 Vac, 90 kVA
Forward E/E Bay

230 Vac Feeder
Generator
2 x 250 kVA

Aft E/E Bay

External Power
2 x 115 Vac, 90 kVA
Loads

Remote Power
Distribution Unit
APU Generator
2 x 225 kVA

www.boeing.com/commercialAeromagazine, aero-quarterly, 04|07

Oliver Meier, Dieter Scholz
Electrical de-icing systems

Deutscher Luft- und Raumfahrtkongress
31.8.2010-02.09.2010 Hamburg

24.08.2010, Folie 3
Aero - Aircraft Design and Systems Group

A HANDBOOK METHOD FOR THE ESTIMATION OF POWER REQUIREMENTS FOR ELECTRICAL DE-ICING SYSTEMS

Aim

- **Estimation of power requirements for electrical de-icing systems**

- Review and improve handbook methods

- Contribution to the preliminary sizing of electrical de-icing systems

- **Simplification of trade-off studies**

Oliver Meier, Dieter Scholz
Electrical de-icing systems

Deutscher Luft- und Raumfahrtkongress
31.8.2010-02.09.2010 Hamburg

24.08.2010, Folie 4
Aero - Aircraft Design and Systems Group

A HANDBOOK METHOD FOR THE ESTIMATION OF POWER REQUIREMENTS FOR ELECTRICAL DE-ICING SYSTEMS

Today's Aircraft Anti-Icing and De-Icing Systems

- **Present System**
  - classically done with **bleed air** taken from the engines
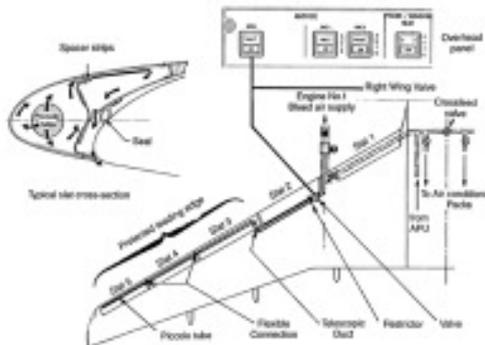
  - **boot surfaces** remove ice accumulations mechanically by alternately inflating and deflating tubes

AIRBUS

FAA: Aircraft Icing Handbook, 1993

Oliver Meier, Dieter Scholz
Electrical de-icing systems

Deutscher Luft- und Raumfahrtkongress
31.8.2010-02.09.2010 Hamburg

24.08.2010, Folie 5
Aero - Aircraft Design and Systems Group
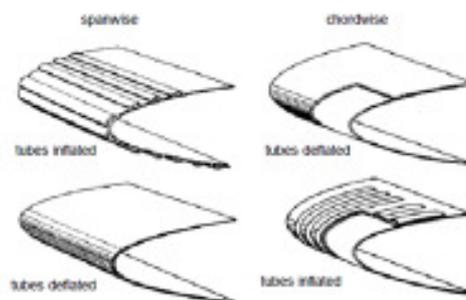
Present and Future Electrical Wing De-Icing Systems

- Electrical power taken from generators on board
- (maybe too) high power demands
- Solution:
  - **Cycling heating** of main surfaces
  - Only **parting strips** permanently heated
- Energy saving:
  - Only melting of ice in contact to surface
  - Most of solid ice carried away by aerodynamic forces
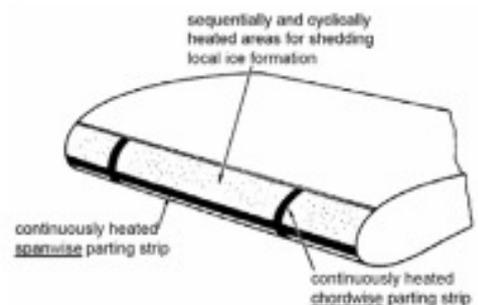
sequentially and cyclically heated areas for shedding local ice formation

continuously heated spanwise parting strip

continuously heated chordwise parting strip

FAA: Aircraft Icing Handbook, 1993

Oliver Meier, Dieter Scholz
Electrical de-icing systems

Deutscher Luft- und Raumfahrtkongress
31.8.2010-02.09.2010 Hamburg

24.08.2010, Folie 6
Aero - Aircraft Design and Systems Group

A HANDBOOK METHOD FOR THE ESTIMATION OF POWER REQUIREMENTS FOR ELECTRICAL DE-ICING SYSTEMS

State-of-the Art Handbook Method

- SAE: *Ice, Rain, Fog and Frost Protection*, 1990 (AIR 1168/4)
  - Mainly based on empirical equations
  - Imperial Units

- Necessity:
  - International approach
  - Equation from thermodynamic first principals
  - SI units

Oliver Meier, Dieter Scholz
Electrical de-icing systems

Deutscher Luft- und Raumfahrtkongress
31.8.2010-02.09.2010 Hamburg

24.08.2010, Folie 7
Aero - Aircraft Design and Systems Group

A HANDBOOK METHOD FOR THE ESTIMATION OF POWER REQUIREMENTS FOR ELECTRICAL DE-ICING SYSTEMS

Assumptions for a Handbook Method

- Selected design point from CS-25:
  - **Temperature**   (0 °F = -17.78 °C)
  - **Liquid water content (LWC)** (guideline from CS-25 2008)
  - **Droplet diameter**   (20µm)
  - **Pressure altitude**   (0 ft)
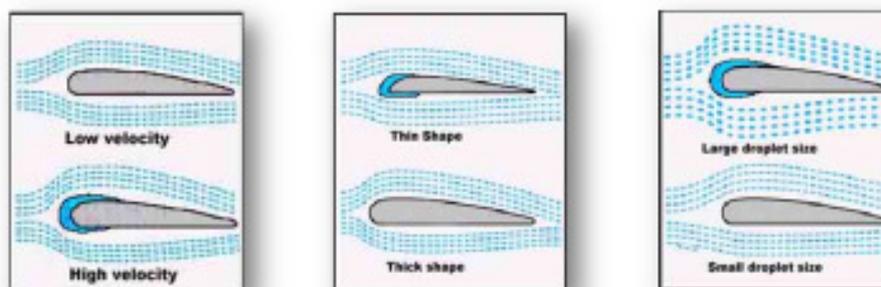
Majed Sammak , Anti-Icing in Gas Turbines, Master Thesis, LUND UNIVERSITY , 2006

Oliver Meier, Dieter Scholz
Electrical de-icing systems

Deutscher Luft- und Raumfahrtkongress
31.8.2010-02.09.2010 Hamburg

24.08.2010, Folie 9
Aero - Aircraft Design and Systems Group

CALCULATION OF POWER REQUIREMENTS

Power Requirements for Continuously Heated Surfaces

- Power requirements calculated from an power balance:

$$\dot{q}_{A/I} = \dot{q}_{latent} + \dot{q}_{sensible} + \dot{q}_{evap} + \dot{q}_{convec} - \dot{q}_{KE} - \dot{q}_{aero}$$
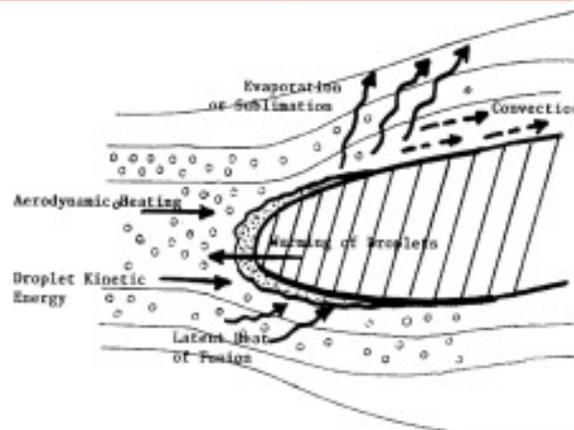
A semi-empirical model for heat transfer and ice accretion on aircraft wings in supercooled clouds,
S.A. Sherif, N. Pasumarthi, C.S. Bartlett,
University of Florida, 1997

Oliver Meier, Dieter Scholz
Electrical de-icing systems

Deutscher Luft- und Raumfahrtkongress
31.8.2010-02.09.2010 Hamburg

24.08.2010, Folie 10
Aero - Aircraft Design and Systems Group

CALCULATION OF POWER REQUIREMENTS

Power Requirements for Continuously Heated Surfaces

- The power balance consists of:
    - **Latent** heat   (ice to water)
    - **Sensible** heat   (water to surface temperature)
    - **Evaporation**   (in a running-wet system)
    - **Convective** cooling   (airflow over surface)
  - ❖ **Kinetic** heating   (impinging droplets)
  - ❖ **Aerodynamic** heating (friction in boundary layer)

source	$\dot{q}_{FS}$ [kW/m²]
Example Calculation for parting strip power Requirements	17.43
AIR 1168/4 calculation scheme	14.13
AIR 1168/4 suggested value (p. 28)	18.6

Oliver Meier, Dieter Scholz
Electrical de-icing systems

Deutscher Luft- und Raumfahrtkongress
31.8.2010-02.09.2010 Hamburg

24.08.2010, Folie 11
Aero - Aircraft Design and Systems Group

CALCULATION OF POWER REQUIREMENTS

Power Requirements for Cyclically Heated Surfaces

- Zones are heated up sequential in a row
- Assumptions:
  - **Ice accretions are allowed to a certain degree**
  - equilibrium temperature = ambient temperature
  - Amount of ice to be melted to destroy the bond between ice and the surface: 0.6mm
  - Heating efficiency is assumed to be 70%.

source	q_{opt} [kW/m²]
Calculated	32.69
AIR 1168/4 (p. 28)	34.10

- The calculated value is not dependent on any aircraft parameters.

Oliver Meier, Dieter Scholz
Electrical de-icing systems

Deutscher Luft- und Raumfahrtkongress
31.8.2010-02.09.2010 Hamburg

24.08.2010, Folie 12
Aero - Aircraft Design and Systems Group

A HANDBOOK METHOD FOR THE ESTIMATION OF POWER REQUIREMENTS FOR ELECTRICAL DE-ICING SYSTEMS

Assumptions for a Handbook Method

- Only two dimensional effects are considered
- Only one point along the airfoil's leading edge is evaluated (average values used)
- Certification rules from CS-25 required but only one design point that is considered critical is taken into account

$$m_{ice}' = v \cdot t \cdot b_{ice} \cdot \rho_{LWC} \cdot E_m$$

$$S_{ice} = t \cdot b_{ice}$$
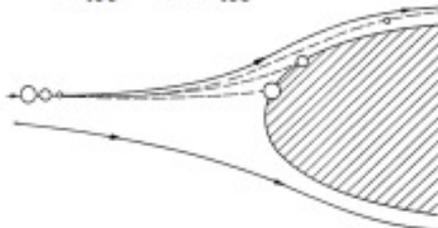
SAE: Ice, Rain, Fog, and Frost Protection, AIR 1168/4, 1990

Oliver Meier, Dieter Scholz
Electrical de-icing systems

Deutscher Luft- und Raumfahrtkongress
31.8.2010-02.09.2010 Hamburg

24.08.2010, Folie 8
Aero - Aircraft Design and Systems Group
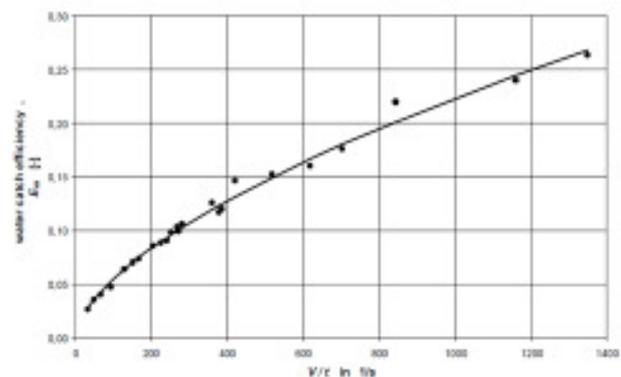
CALCULATION OF POWER REQUIREMENTS

Power Requirements for Generic Heater Layout

- cyclic de-icing uses two basic principles
  - Decrease of the continuous heated area   (*parting strips*)
  - Decrease of the heat-on time   (*cyclic de-icing*)

- k_{PS} gives the ratio of continuously heated parting strips against total heated area Here: **22%**
- k_{cycl} gives the ratio of cyclic heat on time against total cycle time.   Here: **5%**

- Hence: $\dot{q}_{total} = \dot{q}_{PS} \cdot k_{PS} + \dot{q}_{cycl} \cdot k_{cycl}$

  - With k-factors as given above
  - $\dot{q}_{PS} =$ **17.43 kW/m²**
  - $\dot{q}_{cycl} =$ **32.69 kW/m²**
  - The average heat load $\dot{q}_{total} =$ **5.5 kW/m²**

A HANDBOOK METHOD FOR THE ESTIMATION OF POWER REQUIREMENTS FOR ELECTRICAL DE-ICING SYSTEMS

Conclusion

- Calculated specific power requirements are in **good agreement with AIR 1168/4** results under the chosen assumptions

- Handbook Method allows **quick calculation of** specific de-icing **power requirements**
  1. use of given specific power requirements $\dot{q}_{total}$ (given design point, A320, k-factors)
  2. based on specific power requirements $\dot{q}_{total}$ calculated from
     a) individual design point (CS-25) and
     b) individual aircraft parameters
     c) individual k factors describing the heater layout

- Handbook Method with k-factors allows a **description of heater layouts**
  - with de-icing sequence (ratio of on time against cyclic heating period)
  - with specific parting strip area (ratio of parting strip area against total heating area)

A HANDBOOK METHOD FOR THE ESTIMATION OF POWER REQUIREMENTS FOR ELECTRICAL DE-ICING SYSTEMS

Absolute Power Requirements for De-Icing

- Absolute power requirements are based on $S_{ice} = t \cdot b_{ice}$

- Required power: $P_{req} = \dot{q}_{total} \cdot S_{ice}$

- Required power for electrical de-icing of A320
  - 3 heated slats with $b_{ice} = 15,2$ m
  - Chord at middle slat (slat 4): c = 2,5 m
  - $S_{ice} = 37,2$ m²

  $P_{req} = 200 kVA$

- Available electrical power of A320 with one 90 kVA generator on each engine:

  $P_{elec} = 180 kVA$

Oliver Meier, Dieter Scholz
Electrical de-icing systems

Deutscher Luft- und Raumfahrtkongress
31.8.2010-02.09.2010 Hamburg

24.08.2010, Folie 14
Aero - Aircraft Design and Systems Group

A HANDBOOK METHOD FOR THE ESTIMATION OF POWER REQUIREMENTS FOR ELECTRICAL DE-ICING SYSTEMS

Contact

Oliver.Meier@HAW-Hamburg.de

info@profscholz.de

Oliver Meier, Dieter Scholz
Electrical de-icing systems

Deutscher Luft- und Raumfahrtkongress
31.8.2010-02.09.2010 Hamburg

24.08.2010, Folie 16
Aero - Aircraft Design and Systems Group

Appendix C –

CANISE Versions
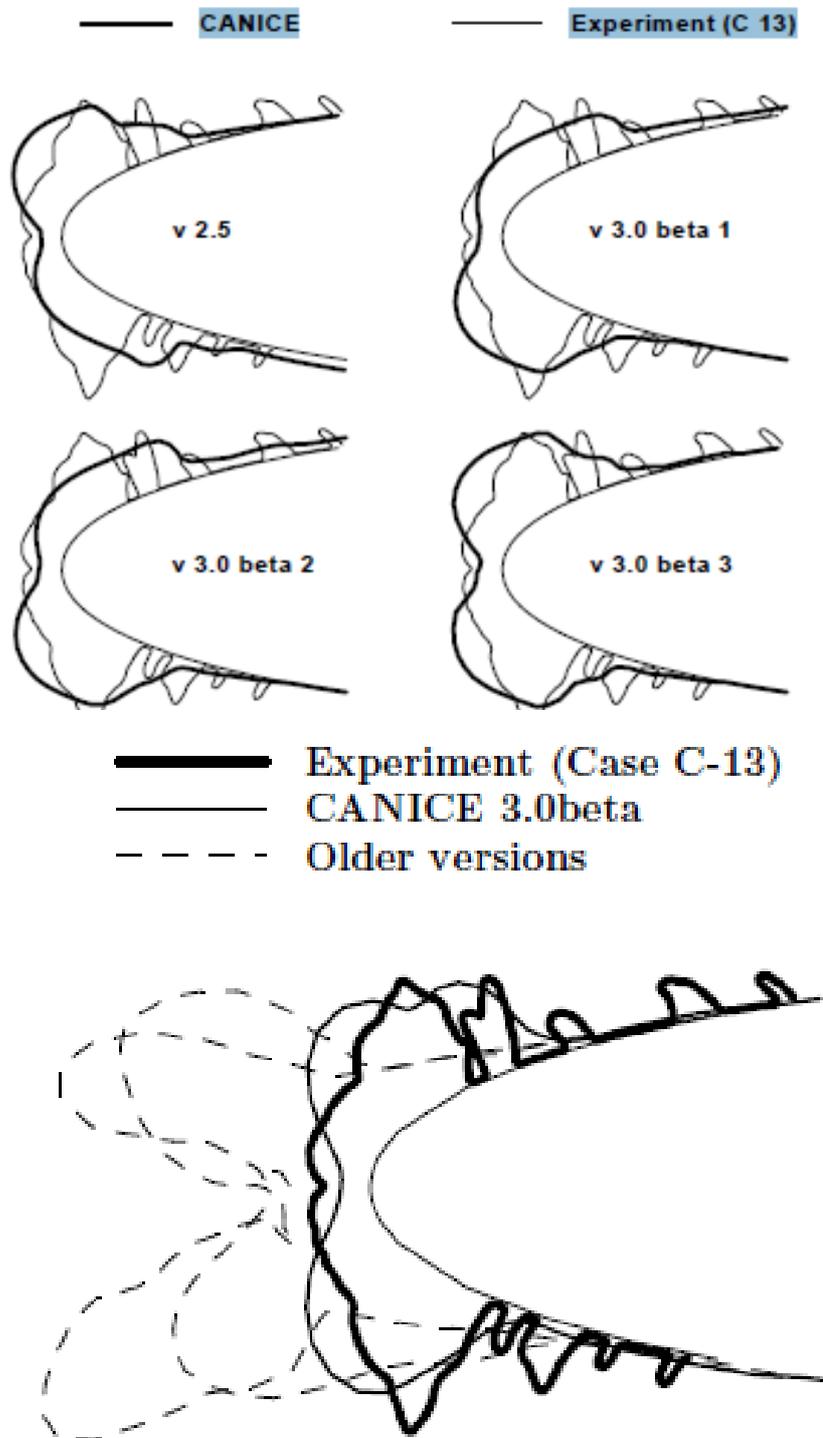
Figure C 4   CANISE code improvement
                (BRAGG 2002)

Appendix D –

Geometry Report B787
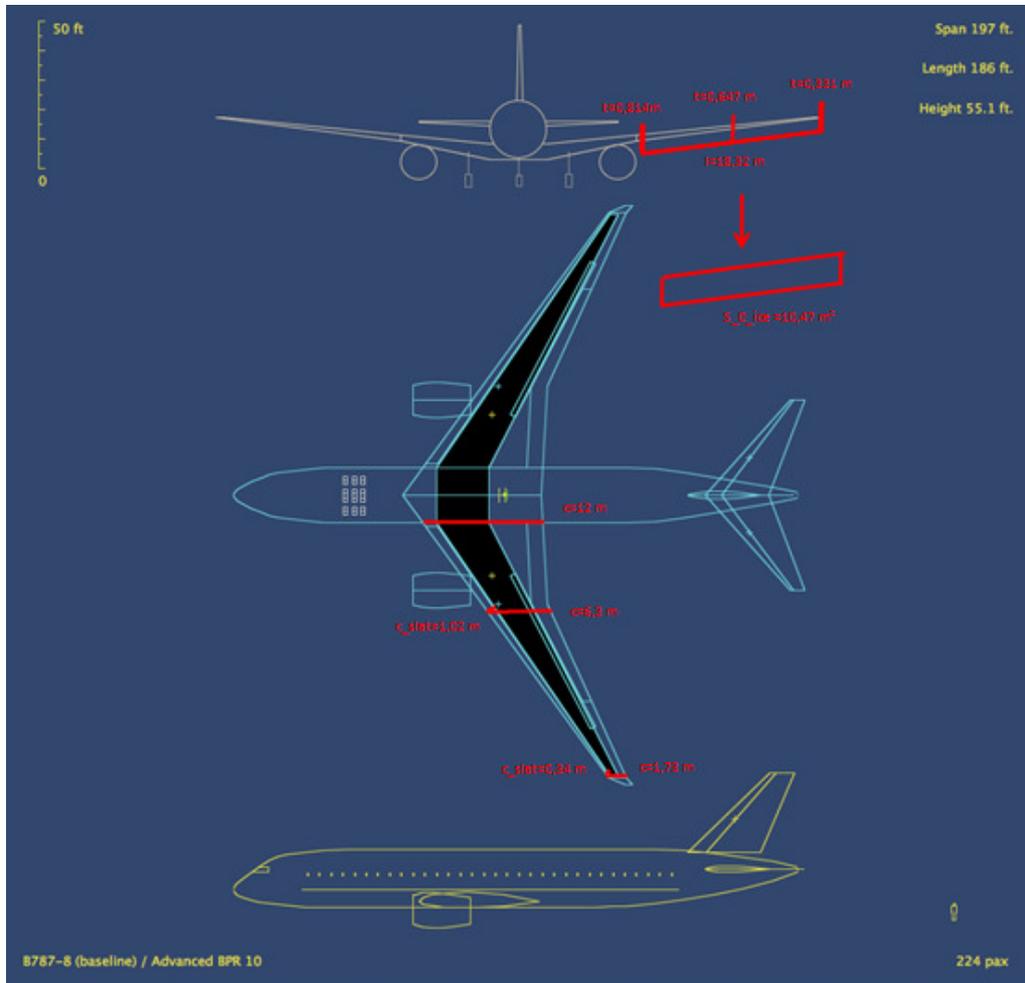
Figure D 5   B787 geometry with simulated icing sieve

GEOMETRY REPORT	Wing	Stabiliser	Fin	
Area, trapezoidal reference	3501.39	832.50	427.50	sq.feet
Area, piano gross	4028.47	832.50	427.50	sq.feet
Area, airbus gross	3971.42			sq.feet
Area, boeing wimpress	3870.00			sq.feet
Area, esdu	3862.65			sq.feet
Area, exposed	3238.14	636.15	427.50	sq.feet
Area, wetted	6591.18	1292.43	868.52	sq.feet
Aspect Ratio, trapezoidal	10.58	5.00	1.70	
Aspect Ratio, piano gross	9.20	5.00	1.70	
Aspect Ratio, airbus gross	9.33			
Aspect Ratio, boeing wimpress	9.58			
Aspect Ratio, esdu	9.59			
Span (excluding winglets)	192.50	64.52	26.96	feet
Sweepback at 1/4-chord	32.20	36.00	40.00	degrees
Taper Ratio (trapezoidal)	0.18	0.22	0.33	
t/c at root	0.134	0.100	0.100	
t/c at thickness break	0.094			
t/c at tip	0.088	0.100	0.100	
Volume Coefficient (V-bar)		0.921	0.049	
Mean Aero Chord (trap.wing)	21.12	14.66	17.18	feet
Arm between MAC 1/4 chords		81.81	77.04	feet
Wing chord at tip			5.55	feet
Wing chord at planform break			21.06	feet
Wing chord at root (gross)			38.94	feet
Wing chord at c/line (gross)			45.00	feet
Wing chord at c/line (notional trapezoidal)			30.83	feet
S_Ice (gesamte zu enteisende Flāche)	20,94			sq.metres

Figure D 2   B787 geometry data

Appendix E –

Excelsheet: Calculation of De-Icing Power
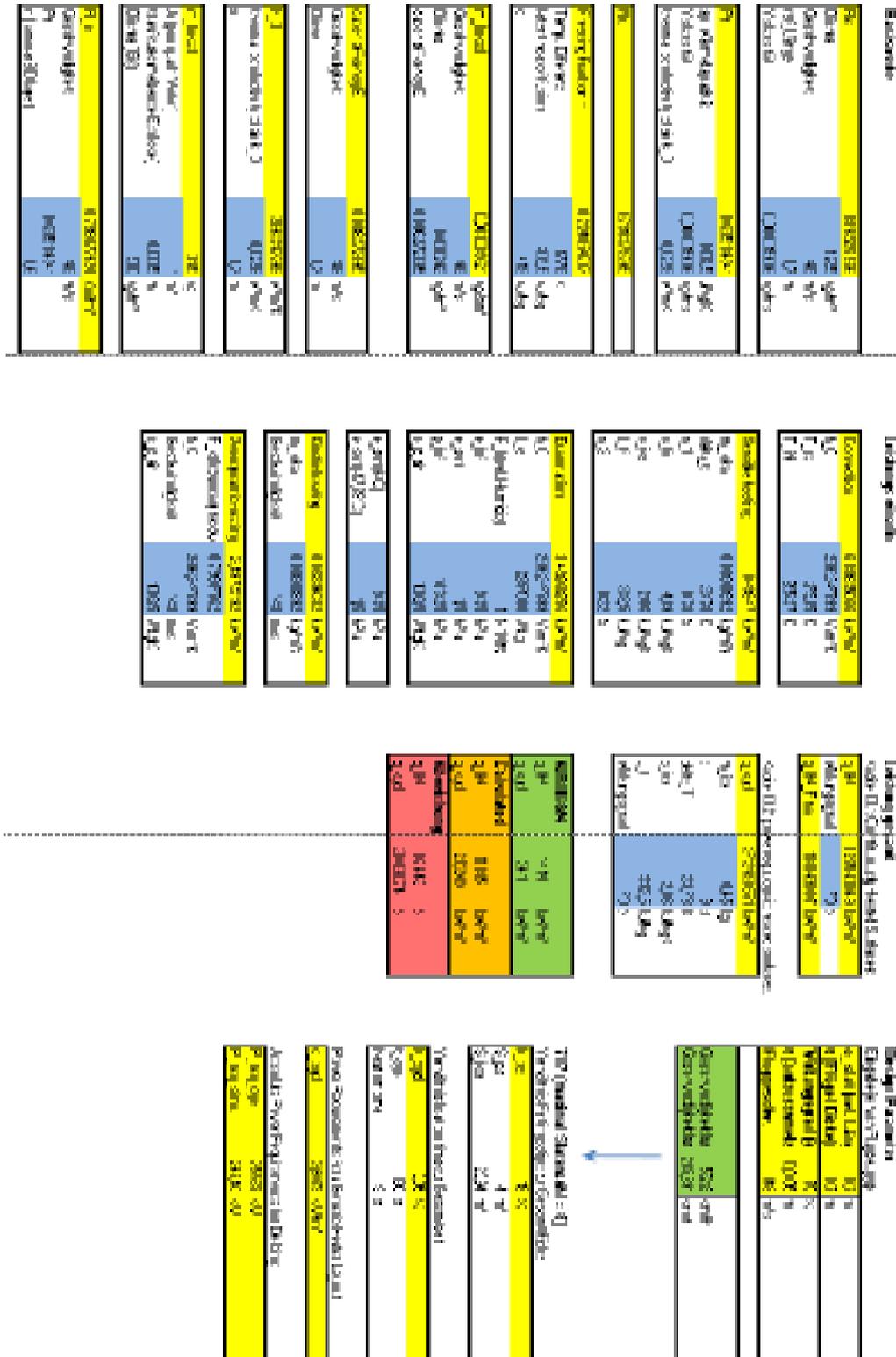
Figure E 6   Calculation scheme with gathered results